



Titre: Title:	Development of Alternative Bacteria Sensing Means	
Auteur: Author:	Narges Emami	
Date:	2021	
Type:	Mémoire ou thèse / Dissertation or Thesis	
Référence: Citation:	Emami, N. (2021). Development of Alternative Bacteria Sensing Means [Master's thesis, Polytechnique Montréal]. PolyPublie. https://publications.polymtl.ca/5624/	

Document en libre accès dans PolyPublie Open Access document in PolyPublie

URL de PolyPublie: PolyPublie URL:	https://publications.polymtl.ca/5624/
Directeurs de recherche: Advisors:	Abdellah Ajji
Programme: Program:	Génie chimique

POLYTECHNIQUE MONTRÉAL

affiliée à l'Université de Montréal

Development of Alternative Bacteria Sensing Means

NARGES EMAMI

Département de génie chimique

Mémoire présenté en vue de l'obtention du diplôme de *Maîtrise ès sciences appliquées*Génie chimique

Janvier 2021

© Narges Emami, 2021.

POLYTECHNIQUE MONTRÉAL

affiliée à l'Université de Montréal

Ce mémoire intitulé :

Development of Alternative Bacteria Sensing Means

présenté par Narges EMAMI

en vue de l'obtention du diplôme de *Maîtrise ès sciences appliquées*a été dûment accepté par le jury d'examen constitué de :

Marie-Claude HEUZEY, présidente

Abdellah AJJI, membre et directeur de recherche

Amir SAFFAR, membre

DEDICATION

To my father

ACKNOWLEDGEMENTS

I wish to express my sincere gratitude and appreciation to the following people who have provided invaluable assistance during my study:

My supervisor, Prof. Abdellah Ajji, for his consistent support and guidance. I have always considered myself fortunate to be able to conduct my research under his authentic supervision. His infinite patience and genuine empathy towards my health situation is something I will forever remember and be grateful for.

Dr. Bentolhoda Heli, who generously shared her profound knowledge and experience with me. She constantly inspired me with her novel ideas in every step of this research.

Dr. Amir Saffar, who not only blessed me with his unique perspectives but also impressed me with his endless kindness and true humility.

My family and friends for their wise counsel and sympathetic ear.

And to Dr. Molly Warner, my beloved hematologist, who has done everything to keep me healthy and strong during my research.

RÉSUMÉ

Dans la première phase de cette étude, une méthode précédemment établie de synthèse de Carbon Quantum Dots (CQDs) fonctionnalisés au mannose a été utilisée. Le chauffage à sec en une étape du D-mannose en présence de citrate d'ammonium dibasique crée une solution fluorescente avec la capacité exceptionnelle de marquer une bactérie pathogène potentiellement mortelle, Escherichia coli. L'affinité forte et spécifique des protéines FimH qui sont des sous-unités des fimbriae de type 1 exprimées par de nombreuses souches d'E. Coli, envers la structure du mannose, permet la détection d'E. Coli. Cette détection est basée sur la variation de l'intensité de fluorescence d'échantillons contenant différentes concentrations d'E. Coli.

Principalement, la spécificité des Man-CQDs à travers E. coli a été inspectée. Ensuite, la polyvalence du capteur a été déterminée en effectuant les tests de détection sur différentes souches d'E. Coli. La faisabilité d'exploiter le capteur synthétisé a ensuite été examinée en effectuant la détection d'E. Coli dans des échantillons réels tels que l'eau du robinet contaminée, la limonade contaminée et le jus de pomme contaminé.

La deuxième phase de l'étude s'est concentrée sur l'amélioration de la sensibilité du capteur en augmentant sa limite de détection en utilisant le 4-nitrophényl α-D-mannopyranoside comme élément de reconnaissance. Le capteur synthétisé a montré une très forte affinité envers Escherichia coli et a démontré un potentiel de détection même à des niveaux allant jusqu'à 10 cfu/ml.

Pour les deux capteurs, des tests de détection ont été répétés plusieurs fois avec différents lots de capteurs afin d'évaluer leur répétabilité et leur fiabilité.

Dans la phase finale, la possibilité d'appliquer les capteurs mentionnés ci-dessus à des fins d'emballage alimentaire a été discutée et des recommandations avantageuses ont été proposées pour être utilisées pour les futurs développements.

ABSTRACT

In the first phase of this study, a previously established method of synthesizing mannose-functionalized CQDs was employed. The one-step dry heating of D-mannose in presence of ammonium citrate dibasic creates a fluorescent solution with the exceptional ability to label a life-threatening pathogenic bacterium, Escherichia coli. The strong and specific affinity of FimH proteins which are subunits of type 1 fimbriae expressed by numerous strains of E. coli, towards mannose structure, permits detection of E. coli. This detection is based on the variation of fluorescent intensity of samples containing different concentrations of E. coli.

Primarily, the specificity of Man-CQDs through E. coli was inspected. Then the sensor's versatility was figured out by performing the sensing tests on different strains of E. coli. The feasibility of exploiting the synthesized sensor was later examined by conducting E. coli detection in real-life samples such as spiked tap water, lemonade and apple juice.

The second phase of the study was concentrated on enhancing the sensitivity of the sensor by increasing its detection limit using 4-Nitrophenyl α -D-mannopyranoside as the recognition element. The synthesized sensor showed a very high affinity towards Escherichia coli and demonstrated a detection potential even at levels down to 10 cfu/ml.

For both sensors, the detection tests were repeated several times with different batches of sensors to assess their repeatability and reliability.

In the final phase, the possibility of applying the aforementioned sensors for food packaging purposes has been discussed and advantageous recommendations have been proposed to be used for future developments.

TABLE OF CONTENTS

DEDICATION	III
ACKNOWLEDGEMENTS	IV
RÉSUMÉ	V
ABSTRACT	VI
TABLE OF CONTENTS	VII
LIST OF TABLES	IX
LIST OF FIGURES	X
LIST OF SYMBOLS AND ABBREVIATIONS	XIV
CHAPTER 1 INTRODUCTION	1
CHAPTER 2 LITERATURE REVIEW	4
2.1 Pathogenic Bacteria and Associated Risks	4
2.2 Biosensor for Pathogenic Bacteria Detection	5
2.2.1 Current Methods of E. coli Detection	5
2.3 Bacterial Adhesion via Protein-Carbohydrate Interactions	7
2.3.1 D-mannose – FimH	11
2.3.2 Increase affinity	13
2.4 Carbon Quantum Dots	15
2.4.1 Properties	16
2.4.2 Synthesis	16
2.4.3 Applications	17
2.5 Quenching Mechanism	18
CHAPTER 3 EXPERIMENTAL METHODOLOGY	21

3.1	Introduction	21
3.2	Materials	21
3.3	Synthesis of functionalized CQDs	22
3.4	Bacterial growth and assays	23
3.5	Analysis of real samples	23
CHAPT	ER 4 RESULTS	25
4.1	Functionalized CQDs	25
4.2	E. coli labelling Man-CQDs	26
4.3	Repeatability, Reproducibility and Practicability of Man-CQDs	31
4.4	The specificity of Man-CQDs to E. coli	40
4.5	E. coli labelling 4-Nitrophenyl α-D-mannopyranoside-CQDs	42
4.6 manno	Repeatability, Reproducibility and Practicability of 4-Nitrophenyl opyranoside-CQDs	
CHAPT	ER 5 GENERAL DISCUSSION	48
5.1	The necessity of the quenching mechanism	50
CHAPT	ER 6 CONCLUSION AND RECOMMENDATION	54
REFERE	ENCES	55

LIST OF TABLES

Table 2.1 Major adherence	factors used to	facilitate attachment	of microbial	pathogens to	host
tissues					7
Table 2.2 Relative potencies	of a series of ar	ylmannosides in inhi	bition assays o	of FimH	14

LIST OF FIGURES

Figure 2.1 Microbial pathogenesis [30]6
Figure 2.2 Schematic representation of a D-Mannose molecule
Figure 2.3 Shadow-cast electron micrograph of E. coli carrying type P fimbriae. The cell is 0.5µm in diameter
Figure 2.4 The important role of multivalent carbohydrates to interfere with the bacteria attachment to a tissue cell
Figure 2.5 Chemical structures of D-fructose, D-mannose, D-glucose, mannan and hemicellulose (-xylose- β (1,4)-mannose- β (1,4)-glucose- α (1,3)-galactose-)
Figure 2.6 FESEM images of FimH+ cells captured on the filter paper infused with CNFs-mannose
Figure 2.7 The schematic structures of CQDs [59]
Figure 2.8 CQDs and their unique applications [54]
Figure 3.1 Schematic representation of the synthesis of mannose modified carbon quantum dots 22
Figure 3.2 Fluorescence spectra of Man-CQDs (×1) for the detection of E. coli K12 in PBS24
Figure 4.1 The absorption spectrum of Man-CQDs (×1)
Figure 4.2The fluorescence emission spectrum of Man-CQDs (×1)
Figure 4.3 Fluorescence spectra of Man-CQDs (×0.1) for the detection of E. coli K12 in PBS26
Figure 4.4 Fluorescence intensity (at 420nm) of Man-CQDs (0.1×) and E. coli K12 in PBS27
Figure 4.5 Fluorescence spectra of Man-CQDs (×0.1) for the detection of E. coli ATCC 25922 in PBS
Figure 4.6 Fluorescence intensity (at 420nm) of Man-CQDs (0.1×) and E. coli ATCC 25922 in PBS

Figure 4.8 Fluorescence intensity (at 420nm) of Man-CQDs (1×) and E. coli K12 in PBS	Figure 4.7 Fluorescence spectra of both Man-CQDs (×1) and Man-CQDs (×0.1) for the detection
Figure 4.9 Fluorescence intensity (at 420nm) of Man-CQDs (1×) and E. coli K12 in PBS	of E. coli K12 in PBS29
Figure 4.10 Fluorescence spectra of Man-CQDs (×1) for the detection of E. coli K12 in PBS31 Figure 4.11 Fluorescence intensity (at 420nm) of Man-CQDs (1×) and E. coli K12 in PBS32 Figure 4.12 Fluorescence spectra of Man-CQDs (×1) for the detection of E. coli K12 in PBS33 Figure 4.13 Fluorescence intensity (at 420nm) of Man-CQDs (1×) and E. coli K12 in PBS34 Figure 4.14 Fluorescence spectra of Man-CQDs (×1) for the detection of E. coli K12 in PBS34 Figure 4.15 Fluorescence intensity (at 420nm) of Man-CQDs (1×) and E. coli K12 in PBS34 Figure 4.16 Fluorescence spectra of Man-CQDs (×1) for the detection of E. coli K12 in Tap Water; Same day - Same batch	Figure 4.8 Fluorescence intensity (at 420nm) of Man-CQDs (1×) and E. coli K12 in PBS30
Figure 4.11 Fluorescence intensity (at 420nm) of Man-CQDs (1×) and E. coli K12 in PBS32 Figure 4.12 Fluorescence spectra of Man-CQDs (×1) for the detection of E. coli K12 in PBS33 Figure 4.13 Fluorescence intensity (at 420nm) of Man-CQDs (1×) and E. coli K12 in PBS34 Figure 4.14 Fluorescence spectra of Man-CQDs (×1) for the detection of E. coli K12 in PBS34 Figure 4.15 Fluorescence intensity (at 420nm) of Man-CQDs (1×) and E. coli K12 in PBS34 Figure 4.16 Fluorescence spectra of Man-CQDs (×1) for the detection of E. coli K12 in Tap Water; Same day - Same batch	Figure 4.9 Fluorescence intensity (at 420nm) of Man-CQDs (1×) and E. coli K12 in PBS30
Figure 4.12 Fluorescence spectra of Man-CQDs (×1) for the detection of E. coli K12 in PBS33 Figure 4.13 Fluorescence intensity (at 420nm) of Man-CQDs (1×) and E. coli K12 in PBS34 Figure 4.14 Fluorescence spectra of Man-CQDs (×1) for the detection of E. coli K12 in PBS34 Figure 4.15 Fluorescence intensity (at 420nm) of Man-CQDs (1×) and E. coli K12 in PBS34 Figure 4.16 Fluorescence spectra of Man-CQDs (×1) for the detection of E. coli K12 in Tap Water; Same day - Same batch	Figure 4.10 Fluorescence spectra of Man-CQDs (\times 1) for the detection of E. coli K12 in PBS31
Figure 4.13 Fluorescence intensity (at 420nm) of Man-CQDs (1×) and E. coli K12 in PBS33 Figure 4.14 Fluorescence spectra of Man-CQDs (×1) for the detection of E. coli K12 in PBS34 Figure 4.15 Fluorescence intensity (at 420nm) of Man-CQDs (1×) and E. coli K12 in PBS34 Figure 4.16 Fluorescence spectra of Man-CQDs (×1) for the detection of E. coli K12 in Tap Water; Same day - Same batch	Figure 4.11 Fluorescence intensity (at 420nm) of Man-CQDs (1×) and E. coli K12 in PBS32
Figure 4.14 Fluorescence spectra of Man-CQDs (×1) for the detection of E. coli K12 in PBS34 Figure 4.15 Fluorescence intensity (at 420nm) of Man-CQDs (1×) and E. coli K12 in PBS34 Figure 4.16 Fluorescence spectra of Man-CQDs (×1) for the detection of E. coli K12 in Tap Water; Same day - Same batch	Figure 4.12 Fluorescence spectra of Man-CQDs (×1) for the detection of E. coli K12 in PBS33
Figure 4.15 Fluorescence intensity (at 420nm) of Man-CQDs (1×) and E. coli K12 in PBS34 Figure 4.16 Fluorescence spectra of Man-CQDs (×1) for the detection of E. coli K12 in Tap Water; Same day - Same batch	Figure 4.13 Fluorescence intensity (at 420nm) of Man-CQDs (1×) and E. coli K12 in PBS33
Figure 4.16 Fluorescence spectra of Man-CQDs (×1) for the detection of E. coli K12 in Tap Water; Same day - Same batch	Figure 4.14 Fluorescence spectra of Man-CQDs (×1) for the detection of E. coli K12 in PBS34
Same day - Same batch	Figure 4.15 Fluorescence intensity (at 420nm) of Man-CQDs (1×) and E. coli K12 in PBS34
Figure 4.17 Fluorescence intensity (at 420nm) of Man-CQDs (1×) and E. coli K12 in Tap Water; Same day - Same batch	
Same day - Same batch	Same day - Same batch
Figure 4.18 Fluorescence spectra of Man-CQDs (×1) for the detection of E. coli K12 in Tap Water; Different days - Same batch	Figure 4.17 Fluorescence intensity (at 420nm) of Man-CQDs (1×) and E. coli K12 in Tap Water
Different days - Same batch	Same day - Same batch
Different days - Same batch	
Juice; Same day - Same batch	
Same day - Same batch	
	Figure 4.22 Fluorescence spectra of Man-CQDs (×1) for the detection of E. coli K12 in Lemonade Same day - Same batch

Figure 4.23 Fluorescence intensity (at 420nm) of Man-CQDs (1×) and E. coli K12 in Lemonade
Same day - Same batch
Figure 4.24 Fluorescence intensity (at 420nm) of Man-CQDs (1×) and E. coli K12 with and without free mannose
Figure 4.25 Fluorescence intensity (at 420nm) of Man-CQDs (1×) and E. coli K12 with and without free sucrose
Figure 4.26 Fluorescence spectra of 4-Nitrophenyl α-D-mannopyranoside-CQDs for the detection of E. coli K12 in PBS; Same day - Same batch
Figure 4.27 Fluorescence intensity (at 420nm) of 4-Nitrophenyl α-D-mannopyranoside-CQDs and E. coli K12 in PBS; Same day - Same batch
Figure 4.28 Fluorescence intensity (at 420nm) of 4-Nitrophenyl α-D-mannopyranoside-CQDs and E. coli K12 in PBS; Same day - Same batch
Figure 4.29 Fluorescence spectra of 4-Nitrophenyl α-D-mannopyranoside-CQDs for the detection of E. coli K12 in Tap Water. Same day - Same batch
Figure 4.30 Fluorescence intensity (at 420nm) of 4-Nitrophenyl α-D-mannopyranoside-CQDs and E. coli K12 in Tap Water. Same day - Same batch
Figure 4.31 Fluorescence spectra of 4-Nitrophenyl α-D-mannopyranoside-CQDs for the detection of E. coli K12 in Apple Juice. Same day - Same batch
Figure 4.32 Fluorescence intensity (at 420nm) of 4-Nitrophenyl α-D-mannopyranoside-CQDs and E. coli K12 in Apple Juice. Same day - Same batch
Figure 4.33 Fluorescence spectra of 4-Nitrophenyl α-D-mannopyranoside-CQDs for the detection of E. coli K12 in Lemonade. Same day - Same batch
Figure 4.34 Fluorescence intensity (at 420nm) of 4-Nitrophenyl α-D-mannopyranoside-CQDs and E. coli K12 in Lemonade. Same day - Same batch
Figure 5.1 Detection mechanism in a liquid-based probe a) sample 1: detection procedure for a sample containing a higher concentration of E. coli. b) sample 2: detection procedure for a sample containing a lower concentration of E. coli.

Figure 5.2 Detection mechanism in a solid-based probe a) sample 1: detection procedure for a
sample containing a higher concentration of E. coli. b) sample 2: detection procedure for a
sample containing a lower concentration of E. coli
Figure 5.3 Detection mechanism in a solid-based probe with quenching mechanism a) sample 1:
detection procedure for a sample containing a higher concentration of E. coli. b) sample 2:
detection procedure for a sample containing a lower concentration of E. coli

LIST OF SYMBOLS AND ABBREVIATIONS

4-Nitrophenyl α -D-mannopyranoside-CQDs: 4-Nitrophenyl α -D-mannopyranoside functionalized

Carbon quantum dots

ATCC: American type culture collection

CFU: Colony forming units

CDC: Disease Control and Prevention

CDs: Carbon dots

CE: Capillary electrophoresis

CQDs: Carbon quantum dots

DET: Dexter energy transfer

E. coli: Escherichia coli

EHEC: Enterohemorrhagic Escherichia coli

ELISA: Enzyme-linked immunoassay

FRET: Förster resonance energy transfer

HCl: Hydrogen chloride

HUS: Haemolytic Uraemic Syndrome

IFE: Inner filter effect

KCl: Potassium chloride

LB: Lysogeny Broth

LOD: Limit of detection

Man-CQDs: Mannose functionalized Carbon quantum dots

Na₂HPO₄: Disodium phosphate

NaCl: Sodium Chloride

NMR: Nuclear magnetic resonance

OD: Optical density

Opa: Opacity associated protein

PBS: Phosphate-buffered saline

PCR: Polymerase chain reaction

PET: Photoinduced electron transfer

QCM: Quartz crystal microbalance

RPM: Round per minute

SET: Surface energy transfer

SPAAN: Software for prediction of adhesins and adhesin-like proteins using neural networks

SRP: Surface plasmon resonance

TNP: 2,4,6-trinitrophenol

WHO: World health organization

CHAPTER 1 INTRODUCTION

It is widely acknowledged how severe pathogenic bacteria can affect human health. Due to the modern lifestyle and changes in food consumption and nutrient intake, the risk of being exposed to these biohazards has been significantly increased. There are some existing ways to detect the presence of bacteria, however, all of them require a great amount of time, significant expenses and unfortunately cannot be done by untrained individuals. E. coli is one of the best-known pathogenic bacteria as it is very common and relatively dangerous. Since the infectious doses of E. coli in food samples is proportionally low, there is an urgent need to develop a rapid, accurate and reliable method to detect these bacteria, display the results and eventually prevent the population from consuming a health-threatening product.

Currently, Enterohaemorrhagic Escherichia coli (EHEC) has been one of the most disquieting foodborne pathogenic bacteria all around the world. Getting affected by EHEC infection can develop Haemolytic Uraemic Syndrome (HUS), a disease that can destroy blood cells, initiating kidney failure and in severe cases, causing death. Among different EHEC strains, E. coli O157:H7 is the most prevalent. According to the Center for Disease Control and Prevention (CDC), almost 73,000 cases of infection and 61 deaths affiliated with E. coli O157:H7 occur in the United States annually [1]. The types of E. coli that can cause illness can be transmitted through contaminated water or food, or contact with people or animals [2].

Some actual techniques are presently used for the detection of E. coli. These methods include polymerase chain reaction (PCR) and SPR, DNA probes and microarray, fluorescently labelled antibodies, fluorescently labelled polymers, fluorescence microarrays and carbohydrate functionalized nanodots as well as the standard method to count E. coli which is selective plate counting. The majority of these techniques are based on selective bacteria growth which is time-consuming. The more rapid ones, unfortunately, require expensive material, specialized storage and a perfectly competent operator [3].

Natural phenomena have always been a great source of inspiration. Through a more detailed observation on a molecular scale, it has been figured out that almost all of the biohazards target the derivative of carbohydrate on the surface of a cell in order to eventually enter it [4]. This tendency to make an attachment between the bacteria and the carbohydrates has opened a new chapter in the science of bacteria detection. It was first distinguished that some sugar residues on cells that line

the surfaces of the body, can function as receptors and facilitate the binding of the body cells to certain human or domestic animal pathogens [5]. This eventually leads to several studies that demonstrate that there is selective binding between the D-mannose and type 1 pilus in E. coli [6].

In the last decades, mannose has been demonstrated to have a great potential as a raw material for biodegradable films either with other polymers or mixed with nanoparticles [7].

Although there have been several studies that validate the selective binding of mannose to type 1 pili in E. coli, there are still so many obstacles in the exploitation of this fact in the actual detection of bacteria. Even in the most recent successful studies, the minimum detectable concentration of E. coli that has been reached is still 100 times more than the life-threatening dosage. There has been a recent work that claims to modify the mannose by a simple two-step reductive amination and lessen the minimum detectable concentration by a few hundred [3], however, it needs to be proved. Another difficulty which has to be taken into account is to display the presence of mannose-E. coli bond in a way that could be observed easily. There have been some attempts to modify mannose with the newly discovered material, carbon quantum dot, in order to induce fluorescent property to mannose [8]. This could be a useful idea. The other obstacle is the substrate which has to be chosen as the base which the target bacteria should be captured on it via mannose bonds. Since developing a biosensor from this method is particularly novel, there is not enough published information about it. The last but not least complication is related to the assembling of the biosensor in the final food packaging. In the case of having food in forms other than liquid, the case will be much more complex since the bacteria will not spread in the sample uniformly. In all existing published studies, there is no work on foods other than juice, water, beer or similarly liquid drinks. The ultimate project goal is to develop a biosensor capable of being further assembled on an appropriate packaging that clearly demonstrates to the consumers whether a food product has been contaminated by pathogenic bacteria such as E. coli or not.

Since being always up-to-date was a basic requirement in this project, a reasonable amount of time had been constantly allocated to literature review. Besides that, the project was divided into several main activities. The first step was about selecting, preparing, and modifying mannose and some strings of bacteria. In the second step, the selectivity of our modified mannose through E. coli as well as some other pathogenic bacteria was investigated. In the next steps, many efforts were made

in order to optimize the detection steps and improve the sensor's accuracy. The feasibility of employing the sensors in practical applications was then examined using real-life contaminated samples. In the final step, a deep, useful study has been done on quenching methods of carbon quantum dots which proposed valuable ideas in order to switch the current application of the sensor from liquid phase only to both liquid and solid substrates.

This thesis is constituted of 5 chapters. Chapter 1 is the introduction which clarifies the main aspects of this study. Chapter 2 will be dedicated to a brief literature review on the principal features related to this study. The importance of developing alternative sensing means for bacteria detection will be demonstrated. This chapter will also explore current bacteria sensing methods and their costs and benefits. Chapter 3 will describe the applied methodology and details on the implementation of the experimental plan. Chapter 4 will present the results obtained in this study as well as a detailed discussion on the necessity of exploiting a quenching mechanism. Chapter 5 will cover the conclusion and will offer beneficial suggestions for future works.

CHAPTER 2 LITERATURE REVIEW

2.1 Pathogenic Bacteria and Associated Risks

Pathogenic bacteria pose a significant threat to humans, animals and agricultural health [9]. The World Health Organization has stated antimicrobial resistance among the 10 most dangerous threats to global health in 2019. Regarding WHO bacterial resistance to current medications have caused humans to become powerless towards the infections. The incapability of preventing infections could subsequently compromise surgery and other treatments such as chemotherapy [10].

Bacteria in general are accountable for 72% of deaths caused by foodborne pathogens while the percentage is 21% for parasites and 7% for viruses. While there are numerous pathogenic bacteria out there, E. coli O157:H7, as well as Salmonella, Listeria and Campylobacter, demonstrate the highest risks to precipitate death [11].

Escherichia coli (E. coli) is a gram-negative, facultatively anaerobic, rod-shaped microorganism and was named after Theodor Escherich who first discovered this bacterium in 1885 [12]. Although both humans and animals can harmlessly become colonized by E. coli as a normal flora, enterohemorrhagic E. coli (EHEC) that is considered as pathogenic E. coli causes severe health problems that may lead to death [13]. Among EHEC serotypes, O157:H7 was first recognized in 1982 after an outbreak of bloody diarrhea in Oregon and Michigan, USA [14, 15]. There have been many more O157:H7 related outbreaks reported worldwide ever since, making E. coli O157:H7 one of the most serious foodborne pathogens out there. Based on data provided by The Centers for Disease Control and Prevention (CDC), E. coli O157:H7 is responsible for 73,000 illnesses, 2,200 hospitalizations and 60 deaths annually in the United States adding 405 million dollars to the medical care expenses each year [11, 16]. The most common way of getting infected by E. coli O157:H7 is through the consumption of contaminated food and water [17].

The facts and statistics associated with pathogenic E. coli which is a major public health concern in North America, Europe and other parts of the world, emphasize the importance of discovering and developing novel tools in order to effectively control this pathogen. Clinical medicine, food safety and environmental surveillance are fundamental practices in order to prevent microbial related diseases [18].

2.2 Biosensor for Pathogenic Bacteria Detection

Since the presence of even a few colonies of pathogenic bacteria can be threatful to human health, discovering rapid and sensitive methods of bacteria detection are in high demand. Sensitivity is also another important requirement for bacteria detectors as pathogenic bacteria often exist in an environment alongside other non-pathogenic microorganisms. Conventional methods of bacterial identification include morphological assessments along with observing the ability of an organism to grow in different environments under varied conditions. These time-consuming techniques can take up to 72 h to collect confirmed results. Traditional techniques for bacterial recognition consist of pre-enrichment, selective enrichment and biochemical screening. These techniques require a relatively complicated series of actions to obtain the final identification results [19]. Polymerase chain reaction (PCR) is another comparably new technology, widely used in order to replicate millions of copies of a bacteria. Although the PCR method is remarkably sensitive, it needs pure samples, consumes hours to process and must be conducted by high expertise individuals [20]. Following the limitation associated with these methods, extensive attempts have been recently pointed towards the development of alternative bacteria sensing means. In order to respond to this demand, different equipment, functioning based on varieties of detection principles such as chromatography, fluorescence spectroscopy, flow cytometry and many others, were introduced. In order to present a proper biosensor, certain properties are highly required. The sensitivity and specificity of a biosensor to distinguish even a single colony of the target bacteria in a multiorganism matrix is the main and most important feature. Another essential characteristic is the potency of a biosensor to directly detect bacteria, even without the need for a pre-enrichment step. Last but not least, these components should be gathered together in a biosensor that responds quickly and functions with a relatively inexpensive and straightforward configuration [21].

2.2.1 Current Methods of E. coli Detection

Selective plate counting, Enzyme-linked immunoassay (ELISA) and PCR are the standard methods used in order to count and investigate pathogenic bacteria such as E. coli [22]. Other currently used techniques to detect E. coli are based on fluorescent-labelled antibodies [23], DNA probes and microarray [24], nanodots carbohydrates [25], fluorescent-labelled polymers [26], fluorescence microarrays [27], PCR and Surface plasmon resonance (SPR) [28]. Selective growth of bacteria is

the fundamental requirement in some of these methods, which means it may take several days to obtain the final result. However, the ones which are more rapid demand for high competence operators and are relatively expensive. With the growing tendency to import raw food from different countries that follow different protocols regarding safety controls, there is an immediate obligation to establish methods that are capable of detecting infectious dose of E. coli. Based on the quantitative risk assessment of a previous outbreak of E. coli O157:H7-associated illness, the threatening amount of Escherichia coli O157:H7 responsible for the infection has been evaluated between 10 to 100 cfu in food samples [29]. The novel method must respond rapidly, function with the least possible sample preparation and be selective and sensitive enough to lessen the potential of obtaining false results [3]. It is always inspiring to carefully observe nature. Phenomena such as microbial pathogenesis which basically refers to the process in which microorganisms bring on diseases [30], demonstrate useful facts that can be positively exploited. One of the most common means by which a variety of bacteria and viruses enter a cell is through the carbohydrate derivatives which are located on that host cell. Bacteria have specific proteins on their surface which enable their attachment to the carbohydrates situated on the cell surface. The carbohydrates could be either simple like mannose (Figure 2.2) or even more complex [31].

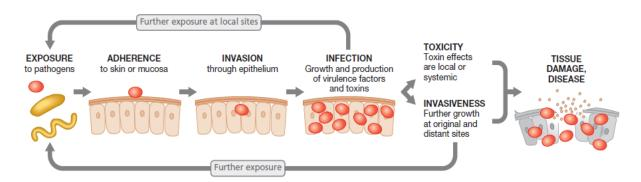


Figure 2.1 Microbial pathogenesis [30]

Figure 2.2 Schematic representation of a D-Mannose molecule

2.3 Bacterial Adhesion via Protein-Carbohydrate Interactions

Bacteria or viruses initiate infectious diseases by adhering to epithelial cells. This adherence takes place due to the specific interaction between molecules on the pathogen and molecules on the host. Although the two most common adherence factors are capsules and slime layers, many pathogens gain entry into specific cells taking advantage of the surface structures of the cell. For instance, Neisseria gonorrhoeae, the pathogenic bacteria which is responsible for one of the most common sexually transmitted diseases named gonorrhea, specifically attach to mucosal cells in the genitourinary tract as well as the rectum, eye and throat while other tissues stay being noninfected. Neisseria gonorrhoeae own surface protein named Opa (opacity associated protein) that specifically targets a molecule on the host called CD66. CD66 can only be found on the surface of these cells and enables the attachment of the pathogenic bacteria to the host cell. Influenzas virus behaves in the same way. This virus particularly binds to lung cells benefiting from the protein hemagglutinin on its surface. Table 2.1 [30] displays useful information about major adherence factors and their examples.

Table 2.1 Major adherence factors used to facilitate attachment of microbial pathogens to host tissues.

Factor	Example
Capsule/slime layer	Pathogenic Escherichia coli—capsule promotes adherence to the brush border of intestinal microvilli Streptococcus mutans—dextran slime layer promotes binding to tooth surfaces
Adherence proteins	Streptococcus pyogenes—M protein on the cell binds to receptors on the respiratory mucosa Neisseria gonorrhoeae—Opa protein on the cell binds to CD66 receptors on the epithelium
Lipoteichoic acid	Streptococcus pyogenes—lipoteichoic acid facilitates binding to the respiratory mucosal receptor (along with M protein)
Fimbriae (pili)	Neisseria gonorrhoeae—pili facilitate binding to epithelium Salmonella species—type I fimbriae facilitate binding to the epithelium of the small intestine Pathogenic Escherichia coli—fimbrial colonization factor antigens (CFAs) facilitate binding to the epithelium of the small intestine

Fimbriae and pili are protein structures located on the bacterial cell surface and play a major role in the binding process. The infection-responsible proteins owned by pathogens are typically part of bacterial appendages [32]. Fimbriated strains of Escherichia coli which are shown in figure 2.3 are more accountable for urinary tract infection than the ones which do not possess fimbriae [30].

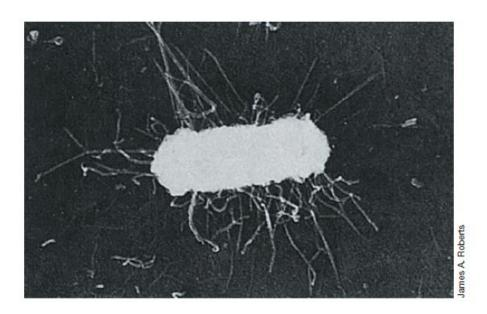


Figure 2.3 Shadow-cast electron micrograph of E. coli carrying type P fimbriae. The cell is $0.5\mu m$ in diameter.

Although the function of both fimbriae and pili is to adhere to host cell surface glycoproteins and inaugurate the attachment process, they differ in the size and distribution aspects. Fimbriae are generally shorter than pili and are found on the pathogen surface to a greater extend. Among various types of fimbriae, type 1 fimbriae which can be found in enteric bacteria such as Escherichia coli, Salmonella and Shigella have been best identified [30].

The attachment of bacteria on the host surface is often assisted by the presented carbohydrates. There are various types of pathogens which are known to function based on protein-carbohydrate adhesion. An available tool is a software program named SPAAN which can be used as a glossary for the pathogens and their related proteins that mediate the host cell attachments [33].

As it has been mentioned previously, the natural affinity of protein structures on the pathogenic bacteria toward a specific carbohydrate on the tissue cell can be used in the biosensor development. Currently, there are limited sensing systems which exploit carbohydrate. The adhesive responsible proteins which are also called lectins are not the products of the immune system in contrast to antibodies. The structure of lectins is various and they particularly bind to carbohydrates. Although Antibodies and DNA may have been better studied in recent years and are most common as recognition elements, they have drawbacks that increase the interest towards utilization of carbohydrates in sensor development. For instance, antibodies are highly unstable and cannot tolerate extreme environments like acidic, basic, organic solvent or high temperature and pressure. The same issue remains while employing nucleic acid assays which also necessitate several purification steps. Carbohydrates are more stable and can remain active under several conditions. Numerous methods can be used in order to detect carbohydrates-protein interactions. These techniques include isothermal titration calorimetry (ITC) [34], surface plasmon resonance (SPR) [35], quartz crystal microbalance (QCM) [36], capillary electrophoresis (CE) [37], nuclear magnetic resonance (NMR) [38] as well as fluorescence spectroscopy [39]. As carbohydrates do not absorb light, in order to assess carbohydrates-protein interaction using optical methods, an additional step of fluorescence labelling of the carbohydrates or proteins should be conducted. Another required step which is currently used in biosensor which acquires carbohydrates as their recognition elements is the immobilization of the carbohydrate on solid surface such as a polymer, glass or quantum dots. Physisorption, covalent immobilization and bio affinity-based interaction are three main strategies in order to immobilize the carbohydrate receptor on the surface of the biosensor [40].

The protein-carbohydrate interaction is a valuable tool to not only be used in sensing applications but also in anti-adhesion strategies. The concept of this strategy is profoundly in demand as it can eventually help reduce the well-known threats of antibiotic resistance. It is basically based on intervention in the early stages of protein-carbohydrate attachment, offering a huge potential to act as an alternative to conventional antibiotics. In the anti-adhesion strategy, free multivalent carbohydrates are being nourished to the system, interfering with the pathogenic attachment and ultimately prevent the pathogen attachment to the tissue cell. The bacteria can be subsequently eliminated by a cleansing mechanism. In this approach, the pathogenic bacteria are turning non-

infective rather than being killed reducing the issues related to harmful by-products discharged from dead bacteria. Figure 2.4 illustrates two scenarios to simplify the plan of action of multivalent carbohydrates in preventing infection [32]. The anti-adhesion approach happens in human bodies on a daily basis. There are many oligosaccharides in human breast milk that function as anti-adhesives [41].

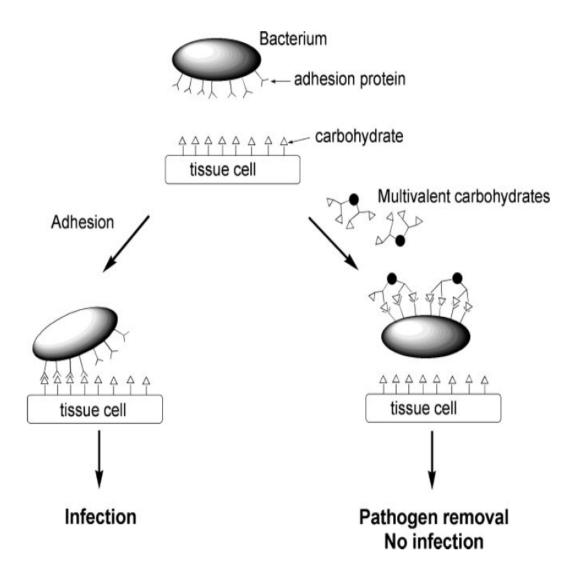


Figure 2.4 The important role of multivalent carbohydrates to interfere with the bacteria attachment to a tissue cell.

2.3.1 D-mannose – FimH

Escherichia coli exhibits some of the most well-characterized adhesins. Urinary tract infection in humans is due to the specific and high affinity of type 1, type P, type S as well as F1C fimbriae towards mannose, Gala1-4Gal (galabiose), sialylated galactose ligands and GalNAcb14Gal epitope respectively [32].

D-mannose is a type of sugar that can be frequently found in foods. It is a C-2 epimer of a well-known natural monosaccharide, D-glucose. Figure 2.5 provides the chemical structure of d-mannose and other similar monosaccharides and carbohydrates. There are several existing sources of mannose. Some plants which are rich in mannose content are peach, aloe vera, corynocarpus, various woods and so many more. Moreover, the cell walls of many microorganisms contain mannans which is one of the most abundant hemicelluloses with mannose being its repeating unit [42].

Figure 2.5 Chemical structures of D-fructose, D-mannose, D-glucose, mannan and hemicellulose (-xylose- β (1,4)-mannose- β (1,4)-glucose- α (1,3)-galactose-).

Thanks to the diverse properties of mannose, it has recently drawn considerable attention both from the food industry as well as the scholarly world. It plays a central role in numerous fields. Potential areas are such as food, medicine, cosmetics, sensing application and feed additives. For instance, Mannose has been already used even commercially in the food industry as a food-texture improver. It is also considered a low-calorie sweetener and a promising alternative to sucrose. An interesting feature of mannose is that unlike other sweeteners its sweetness intensity does not depend on a power function of concentration. It is also noticeably beneficial in medical purposes such as antitumor agents, vitamins and an inexpensive material to be used in drug delivery system production [43, 44]. In 1997, Deckner and Wivell introduced a featured product containing mannose to the cosmetic industry which can act both as a skin-cleanser as well as a moisturizer. As mannose is the most powerful sugar in terms of inhibiting colonization, it is broadly used in animal feeds to assure their intestinal health [42].

The best-studied carbohydrate-protein interaction in pathogenic Escherichia coli is certainly the type 1 mannose-specific fimbriae that include several subunits. The majority of E. coli strains display type 1 fimbriae which are hair-like extensions containing various subunits of FimA and a relatively minor quantity of FimF, FimG and FimH [45]. Genetic and immunological investigation methods have mentioned FimH as the responsible protein to form a specific bind with structures containing D-mannose [46]. Most E. coli fimbriae are located in the fimbrial shaft and their activation is dependent on pilus fragmentation which exposes the binding spots. Whereas in the case of FimH, the proteins are situated at the tip of the fimbriae whether in multiple copies or single forms and make it much simpler to initiate an attachment as well as more accessible for being studied [47, 48].

Recently, Hong Dong et al developed filter papers containing cellulose nano-fibrils functionalized mannose which were efficient in capturing E. coli from liquid systems. FimH-mannose interactions are clearly shown in Figure 2.6 which illustrates Field Emission Scanning Electron Microscope images of FimH containing cells captured by these filter papers [49].

Detailed knowledge of the strong and specific interaction of D-mannose and FimH is essential in order to fully utilize the attachment mechanism for biosensor development purposes.

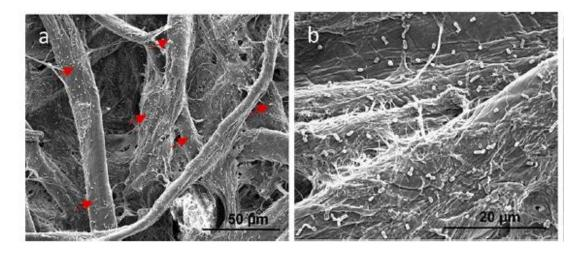


Figure 2.6 FESEM images of FimH+ cells captured on the filter paper infused with CNFs-mannose

2.3.2 Increase affinity

One of the main issues of using carbohydrates as recognition elements in novel biosensors is their relatively weaker bond which they make with the target bacteria. As the infectious dose of pathogenic E. coli in food samples can be as low as 10-100 colony-forming units, presently, one of the main challenges being faced by bio-sensor developers is to improve the affinity of mannose towards E. coli fimbriae. It has been stated in the literature that adding hydrophobic side groups such as phenyl residues or aliphatic chain to mannose effects and boosts its sensitivity to FimH adhesin [50]. Other studies evaluated different derivatives of mannose based on their inhibition performance. Table 2.2 represents the results [51]. Replacing the whole bacteria with the isolated fimbriae did not significantly affect the inhabitation performance of these derivatives of mannose [32]. The majorities of related researches pointed a derivative of mannose, $\rho NP\alpha Man$, as the most potent compound and effective inhibitor [33]. Very limited experimental works have been currently done using $\rho NP\alpha Man$ in bacterial detection but even experimentality, it demonstrated a 50-time better inhibition performance than mannose. In the same study, $\rho NP\alpha Man$ was also functionalized to a fluorescent polymer for labelling Escherichia coli [26].

Table 2.2 Relative potencies of a series of arylmannosides in inhibition assays of FimH

Structures	Inhibition performance/ MeαMan
HO OCH3	1
NO HOLD NO	70
HOO OH OH	150
HO OH OEt	240
HO OH O	470
HO HO OH	1010

2.4 Carbon Quantum Dots

the charges confined in surface flaws [58].

properties and technical applications. Carbon quantum dots, a new member of this family with unique properties and a wide range of applications received so much attention in recent years. With CQDs, Carbon, which is known for its black colour and non-solubility in water, turned into a water-soluble and luminescence nanomaterial. The advantages of carbon quantum dot over other quantum dots in which heavy metals have a major role in their fabrication are non-toxicity and the lower price [52, 53]. The biocompatibility of these nanomaterials made them one of the best alternatives to conventional quantum dots and can be used in many bio-related applications like bio-imaging and biosensing. With the ability to be fluorescent, CQDs made their way to Optronics as well [54]. Like many other discoveries, CQDs were obtained by accident in 2004 by Xu et al. while working on the single-walled carbon nanotubes [55]. This resulted in extensive studies on the fluorescence of the CQDs and the name was given to them by Sun et al. as well as a method to fabricate these quantum dots efficiently [56]. More researches needed to be done on the CQDs' fluorescence emission since the origin of this phenomenon has still remained a mystery. One of the possible explanations endorsed by some researchers is the transition of the electrons between different energy levels [57]. The other researchers have proposed the idea that the fluorescence comes from

Carbon nanomaterials were a point of interest to explore for many researchers due to their unique

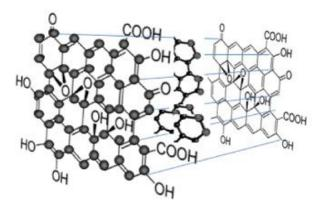


Figure 2.7 The schematic structures of CQDs [59]

2.4.1 Properties

The presence of the high numbers of carboxyl groups in the CQDs' structure made them water-soluble and suitable for biological applications [53]. The luminescence of the CQDs can be improved with some modifications like surface passivation with different substances. Rimal et al.'s work on the CQDs in high temperature (800 °C) demonstrated that the CQDs have the potentials to be used at high-temperature as well [60].

2.4.2 Synthesis

The synthesis of the CQDs can be done in two ways, the "Top-down" and the "Bottom up" [53]. Enhancement and optimization can be done to achieve the desired properties during or after the production of CQDs [54].

2.4.2.1 Top Down

In this method, electrochemical procedures such as Photo ablation or electric arc is recruited to fractionate carbon particles such as graphite and carbon nanotubes into smaller particles like CQDs [53]. Zhou et al. were the first group of researchers who used these methods [61].

2.4.2.2 Bottom Up

On the contrary, the bottom up methods attempt to use smaller molecules such as citrates, carbohydrates and polymer-silica nanocomposites to fabricate CQDs. Thermal modifications make these transitions possible. Liu et al. used silica spheres and resols to produce CQD [62]. Bourlinos' team used ammonium citrate to synthesize the CQD [63]. Zhu et al. synthesized the CQDs by microwave pyrolysis of the Polyethylene glycol (PEG) and saccharide [64].

The trending topic among the researchers is to find green synthesis methods for CQDs [65, 66].

2.4.2.3 Size Control

One of the important steps in producing the CQDs is to modify their size in order to have consistency in properties [54]. This step can be done during or after fabrication. Post-treatment methods consist of filtration, centrifugation and column chromatography [54]. Zhu's team worked on size control during production and achieved uniform CQDs with outstanding properties [64].

2.4.2.4 Modification

Another important step in CQD production is modification. Traditional quantum dots show high quantum yield. Most of the common CQDs showed less than 10% quantum yield and in order to be comparable to the traditional quantum dots, their quantum yield needs to be improved [53]. This improvement can be achieved by surface passivation and doping. Surface passivation is used to eliminate the pollution that contaminates the surface of the CQDs and improve the optical properties of the CQD [67]. For this purpose, the surface of the CQD is modified with acid and then a fine layer of polymer is applied to the surface [53].

2.4.3 Applications

As mentioned before, due to CQDs special properties such as biocompatibility and non-toxicity, they can be used in many bio-related applications such as bioimaging, biosensors and drug delivery [54].

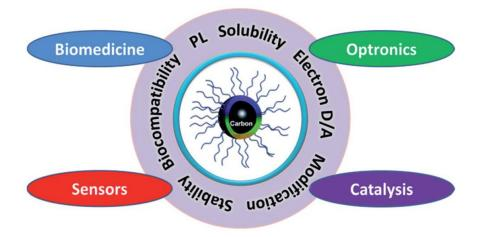


Figure 2.8 CQDs and their unique applications [54]

2.4.3.1 Bioimaging

CQDs can be injected into a living body for imaging. As a case in point, dye conjugated CQDs change colour from blue to green encountering H₂S. So CQDs can picture the fluctuations in physiological amounts of H₂S [53].

2.4.3.2 Drug Delivery

Due to the superior properties of carbon quantum dots, they are currently demanding elements in drug delivery systems. They can be used in various forms. Based on recent studies, the drug can be anchored on the CQDs surface and then be released in the appropriate target area. Also, hollow CQDs have been introduced for drug loading. Other studies have mentioned passivated CQDS for higher loading efficiency and faster diffusion into cells. It can be even used to simultaneously deliver two or more drugs [68].

2.4.3.3 Sensing

Functionalized carbon quantum dots are highly trendy in sensing applications. In chemo sensing, for instance, they are utilized to target heavy metals or small molecules which are biologically-active to increase environmental health and safety [69].

Ning et al proposed a green approach of synthesizing carbon dots from papaya to be further used in biosensing applications such as Iron (III) and Escherichia coli [70].

In another study conducted by Lai et al, solid-state synthesis of functionalizing fluorescent carbon quantum dots has been claimed to be an effective approach to create a biosensor for bacteria and tumour cell bio labelling [71].

2.5 Quenching Mechanism

Fluorescence strength can be diminished by implementing different procedures. The act of reducing fluorescence intensity is called quenching. There are several procedures such as excited-state reactions, molecular rearrangements, energy transfer, ground-state complex formation, and collisional (Dynamic) quenching that can quench a fluorescent material. Chemical compounds such as oxygen, iodide ion and acrylamide have been used commonly as quenchers. Researchers investigated Fluorescence Quenching's nature and they also studied its informative role in the context of bio application. Both static and dynamic quenching is the outcome of the molecular interactions and these interactions make quenching a promising choice in biochemical applications. In the dynamic quenching, diffusion of the quencher into fluorescent happens which results in transferring the excited state to the ground state, thus the emission fades out without any molecular

alteration. In static quenching, the substance produces a nonfluorescent complex upon contact with the quencher. So the contact between the quencher molecules and the fluorophore is the principal of quenching which makes quenching a useful tool in biochemicals [72].

As it was mentioned before, Carbon quantum dots, are carbon-based nanomaterials with a diameter less than 10nm with the ability of photoluminescence and visible emission due to electron excitation [73]. Other properties that make this nanoparticle unique are biocompatibility, non-toxicity and water solubility [74].

In the case of carbon dots (CDs), when they are used for detection, the interaction between the sample and the CDs, which is fluorescent intensity decrease by quenching and increase due to defeating the quenching, has the key role. The processes are used to quench the CDs are static quenching, dynamic quenching, energy transfer, photoinduced electron transfer (PET) and inner filter effect (IFE) [75]. Subcategories of the energy transfer mechanisms are Förster resonance energy transfer (FRET), Dexter energy transfer (DET) and Surface energy transfer (SET). The static and dynamic mechanisms are as explained before. FRET was discovered by Förster, a German scientist, in 1948. The FRET mechanism is the receiving and emitting of photonic energy of the primary fluorophore (donor) by the secondary fluorophore (receiver) in a consecutive manner [76]. In the DET mechanism, instead of the photon, the electron relocation does all the work. SET which is the state of the art in quenching mechanisms requires a metallic surface and a molecular (organic) dipole. IFE is used in the case of convergence of the quencher's absorption spectrum and the emission spectrum of the carbon dots [77].

One of the organics that can be detected using static quenching of the CDs, is dopamine. Dopamine is a neurotransmitter and in the human body, it is used to transfer messages between nerve cells. In a work done by Zhu et al. [78], nano-graphite is used to quench the aptamer-CDs. In the presence of this chemical, the aptamers tend to detach from the CDs and attach to the dopamine, thus the CDs become fluorescent again. The presence of dopamine in human urine can be sensed with this technique.

Purbia et al. [79], quenched the CDs using Cu²⁺ via PET mechanism and it has been observed that the thiamine can recover the fluorescence of the CDs so this method can be implemented to sense the presence of thiamine in blood. Glutathione, which is an antioxidant in our body can be sensed

via FRET quenching. Yang et al. [80], worked on the interactions between CDs and MnO₂ as the quencher. The dominant mechanism here is FRET quenching. The presence of the glutathione recovers the CDs fluorescence. Shi et al. [81] developed a method for detection 2,4,6-trinitrophenol (TNP). TNP could act as a quencher for their sucrose phosphate solution base CDs via the FRET mechanism. The developed technique showed promising results for E-coli labelling and intracellular imaging applications.

Taking into account the presented facts and statistics in this chapter, E. coli can be considered as one of the most life-threatening pathogenic bacteria. Current methods of detecting bacteria are commonly very time-consuming. The techniques which can detect bacteria more rapidly, are expensive and generally require high user expertise. The necessity of developing novel techniques of bacterial detection is indisputable. Bacterial adhesion through protein-carbohydrate interaction has recently drawn lots of attention in different applications such as anti-adhesion mechanisms and biosensing. The specific and strong interaction between mannose and FimH has shown to be a significant potential for E. coli detection purposes. In order to develop a sensitive biosensor capable of detecting even a few colonies forming units of E. coli in a multi organism matrices, this interaction needs to be enhanced. Adding hydrophobic side groups such as phenyl residues or aliphatic chain to mannose boosts its sensitivity to FimH adhesin. Derivatives of mannose have demonstrated a higher affinity towards FimH adhesin. The general objective of this study is to develop a sensor that is able to detect E. coli using protein-carbohydrate interaction. The target concentration is as minimal as 10 cfu/ml. A simple heating method was used to functionalize selected carbohydrates with carbon quantum dots. The fluorescent properties of CQDs along with the high affinity of mannose molecules towards E. coli establish the foundations of our detection technique. Also, a brief review has been done on the quenching mechanism as a recommendation for future works in case the detection is required to be done in solid phases.

CHAPTER 3 EXPERIMENTAL METHODOLOGY

3.1 Introduction

A previously established method [8, 71] was used in this study to synthesis Mannose functionalized carbon quantum dots. The simple one-step dry heating method was later operated to produce 4-Nitrophenyl α-D-mannopyranoside functionalized carbon quantum dots. The aforementioned solutions were capable of selectively targeting FimH adhesin and therefore labelling Escherichia coli. 4-Nitrophenyl α-D-mannopyranoside proved to have a higher affinity towards the target bacteria. The detection tests are based on the fluorescence properties of the prepared solutions. Both Mannose functionalized carbon quantum dots and Nitrophenyl α-D-mannopyranoside functionalized carbon quantum dots exhibit deep indigo fluorescence when getting excited with a UV lamp. We examined the ability of both sensors to detect E. coli at different concentrations from 1.0×10^{1} to 1.0×10^{7} colony forming units (cfu) ml⁻¹. The fluorescence intensity of contaminated solutions being labelled by the sensors reveals to be a function of E. coli concentration as it increases upon the augmentation of E. coli concentration. The practicability of both sensors to be used in real-life contaminated samples was then assessed using tap water, lemonade and apple juice. The specificity of probes towards E. coli was examined as well by nourishing the detection medium with free mannose and free sucrose. Also, different concentrations of the first sensor were prepared by means of evaluating their sensitivity. The detection tests were conducted on two different strains of E. coli possessing different types of fimbriae in order to assess the sensor's versatility. The same detection tests were performed multiple times, on different days, with different batches of sensors to evaluate the repeatability and reliability of both sensors.

3.2 Materials

Ammonium citrate dibasic and 4-Nitrophenyl α-D-mannopyranoside were purchased from Sigma-Aldrich. Mannose was purchased from Thermo Fisher Scientific. Lysogeny Broth (LB) powder was used to prepare LB broth. Two different strains of E. coli were tested in this study; ATCC 25922 which was purchased from The American Type Culture Collection (ATCC) and K12 which was provided by the microbiological department of l'université de Montréal.

3.3 Synthesis of functionalized CQDs

Carbonization of ammonium citrate in solid form with mannose being present in the system has been demonstrated to be a simple yet promising bottom-up method to prepare mannose modified CQDs. 100 mg ammonium citrate and 5 mg mannose were precisely measured, mixed and manually ground in a mortar and pestle for few minutes. This ratio was selected based on a previous study which figured out the optimum ratio of ammonium citrate to mannose to be 20:1 and was repeated in order to reach the highest labelling efficiency[8]. The mixture was poured into a beaker, placed in a furnace and heated at 180 °C for 2 hours. The high heat visually transformed the white mixture into a black residue which was kept at room temperature for a few hours to cool down. It was then dissolved in 10 ml of NaOH solution (0.1M). Post treatments are essentials steps in order to control the size of CQDs and uniform properties. Accordingly, the solution was sonicated for 1 hour and later centrifuged (Desaga sarstedt-gruppe MC2 centrifuge) at 13000 RPM for 1h. These steps are important to remove large particles. Lastly, the solution was dialyzed through a dialysis membrane (MCWO 0.5-1 kd; Float-A-Lyzer G2) for 5 hours with Milli-Q water being replaced every hour. The concentration of this probe was denoted as 1× and henceforth will be referred to as sensor 1. The same procedure was followed to synthesize 4-Nitrophenyl α -D-mannopyranoside modified CQDs with the ratio of ammonium citrate to 4-Nitrophenyl α-D-mannopyranoside stays the same 20:1. This probe will further be referred to as sensor 2. Both sensors were stored at 4 °C.

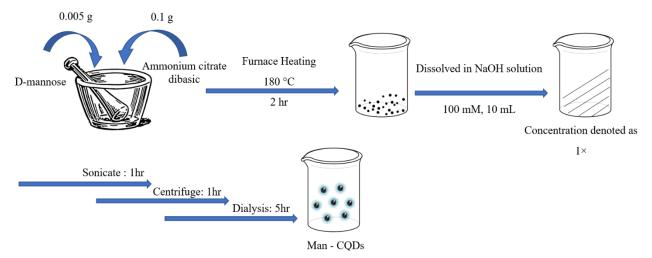


Figure 3.1 Schematic representation of the synthesis of mannose modified carbon quantum dots

3.4 Bacterial growth and assays

Bacterial culturing and sample handling were carried out in a sterile clean room. All apparatus was autoclaved at a high temperature prior to use in order to ensure sterilization. To culture, the desired bacteria, single colonies of E. coli ATCC 25922 and E. coli K12 were lifted from their own LB agar and separately inoculated in LB broth. The bacterial inoculums were grown at 37 °C with a shaking speed of 200 rpm until the absorbance at 600 nm (OD₆₀₀) reached 1.0. 1 ml of each cell mixture was then centrifuged at 8000 RPM for 3 min and washed twice with phosphate-buffered saline (PBS, 10 mM Na2HPO4, 140 mM NaCl, and 2.70 mM KCl; adjusted to pH 7.4 using HCl; 1 mL). The cells were diluted to a concentration of 1.0×10^1 to 1.0×10^7 cfu/ml and incubated with the desired sensor. The incubation with either Man-CQDs or 4-Nitrophenyl α -D-mannopyranoside-CQDs took place for 1 hour and under gentle shaking at room temperature. The mixture was subsequently centrifuged at 13000 RPM for 20 min. The bacterial residue was resuspended in PBS. The final samples were transferred into Costar 96-well black polystyrene plate for fluorescence spectra. A fluorescence intensity scan was conducted by Microplate Tecan Infinite M200 with an excitation wavelength of 340 nm. Figure 3.2 shows typical fluorescence signal result.

3.5 Analysis of real samples

For real sample analysis, tap water, apple juice and lemonade were used. The same practical procedure was basically used. A standard method of culturing the bacterial inoculum overnight at 37 °C with a shaking speed of 200 rpm until the absorbance at 600 nm (OD_{600}) reached 1.0 was carried out. As explained previously, 1 ml of the cell mixture was centrifuged and washed twice. The bacterial pellets were then resuspended in tap water, apple juice and lemonade. The contaminated liquids were then diluted to a concentration of 1.0×10^1 to 1.0×10^7 cfu/ml, incubated with either of the sensors under the same condition and centrifuged for the same duration. The residue was resuspended in tap water, apple juice and lemonade respectively.

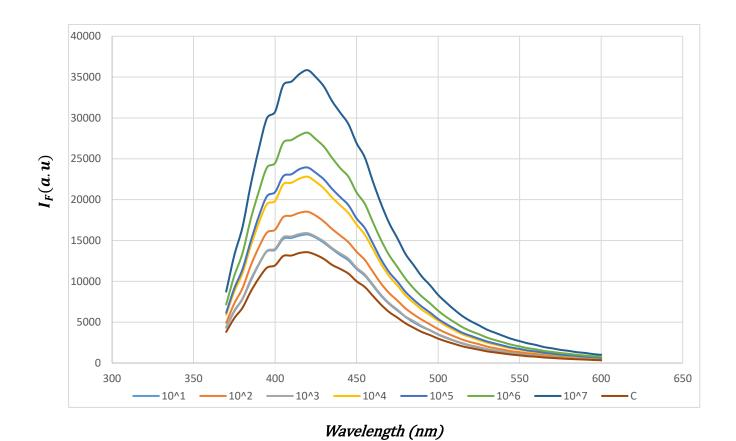


Figure 3.2 Fluorescence spectra of Man-CQDs (×1) for the detection of E. coli K12 in PBS

.

CHAPTER 4 RESULTS

4.1 Functionalized CQDs

It has not been yet comprehensively figured out how mannose modify the carbon quantum dots in the forming process. It is assumed that the mannose molecules were held securely on the soft surfaces of CQDs. Although more or less the possibility of covalent binding of mannose to CQDs can not be excluded, it is more believed that the above-mentioned dehydration reaction led the mannose units to become physically adsorbed and directly anchored on CQDs.

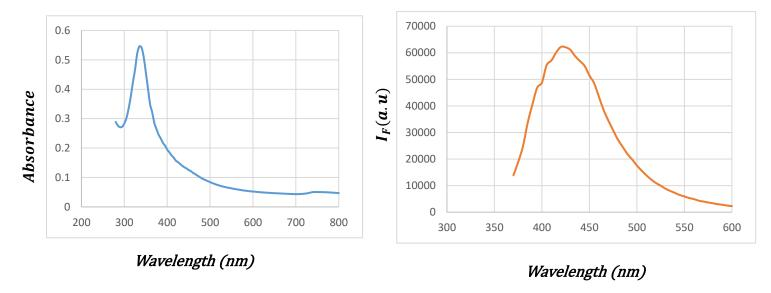


Figure 4.1 The absorption spectrum of Man-CQDs (×1)

Figure 4.2The fluorescence emission spectrum of Man-CQDs (×1)

To better characterize the synthesized sensors, the absorption spectrum, as well as the fluorescence emission spectrum tests, were operated on them. Figure 4.1 displays the absorption spectrum of Man-CQDs (×1) while Figure 4.2 illustrates its fluorescence emission spectrum. The maximum absorption can be observed at 340 nm. Sensor 1 gets excited at 340 nm and emits at 420 nm which signify a strong fluorescence.

4.2 E. coli labelling Man-CQDs

The intense fluorescence properties of our synthesized sensor alongside the inclination of mannose units towards FimH adhesins, make Man-CQDs a suitable probe to be used for E. coli detection purposes. In this study, the detection tests were carried out on two strains of Escherichia coli. E. coli K12 possesses mannose-specific fimbriae while E. coli ATCC 25922 does not express sufficient wild-type 1 fimbriae. Different concentrations of each bacterial suspensions were incubated with Man-CQDs (\times 0.1) at room temperature for 1 hr under gentle shaking. The suspensions were then centrifuged and washed with PBS and the remaining bacterial pellets were resuspended in PBS for further investigation.

Escherichia coli K12

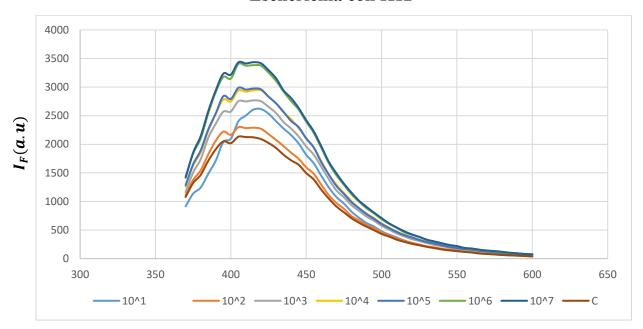


Figure 4.3 Fluorescence spectra of Man-CQDs (×0.1) for the detection of E. coli K12 in PBS

Escherichia coli K12

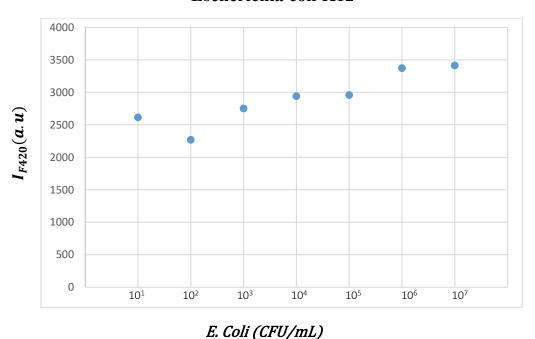
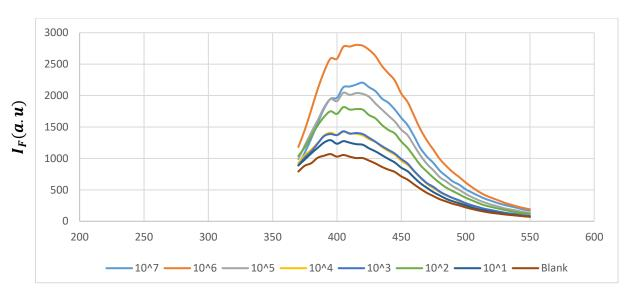


Figure 4.4 Fluorescence intensity (at 420nm) of Man-CQDs (0.1×) and E. coli K12 in PBS

The fluorescence spectra of Man-CQDs ($\times 0.1$) used as a probe to detect E. coli K12 which is presented in figure 4.3 reveal that the fluorescence increased upon increasing the concentration of E. coli. Figure 4.4 displays the fluorescence intensity of Man-CQDs ($0.1\times$) as a function of E. coli K12 concentration at 420nm. Although unpredictable results were observed for the concentrations below 1.0×10^3 , the general trend was acceptable above 100 cfu.

This pattern was not achieved when the detection tests were conducted with E. coli ATCC 25922. The detection tests were also carried out with Man-CQDs $(0.1\times)$ as the probe. Figure 4.5 represents the fluorescence spectra and Figure 4.6 demonstrates the fluorescence intensity of Man-CQDs $(0.1\times)$ as a function of E. coli ATCC 25922 concentration at 420nm. As discussed earlier in chapter 2, not all the strains of E. coli possess adequate FimH adhesin which is responsible for mannose-binding. The following results verified our assumption that our sensor functions based on carbohydrates-protein adhesion and that Man-CQDs selectively attaches to FimH proteins in the target E. coli.

Escherichia coli ATCC 25922



Wavelength (nm)

Figure 4.5 Fluorescence spectra of Man-CQDs $(\times 0.1)$ for the detection of E. coli ATCC 25922 in PBS

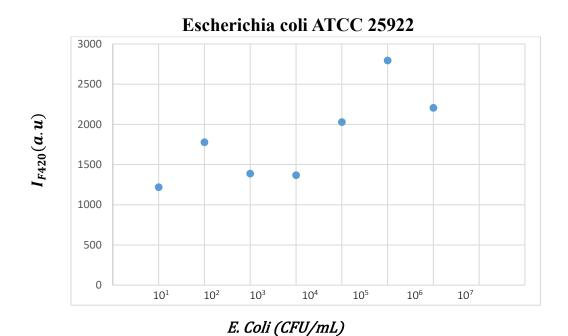
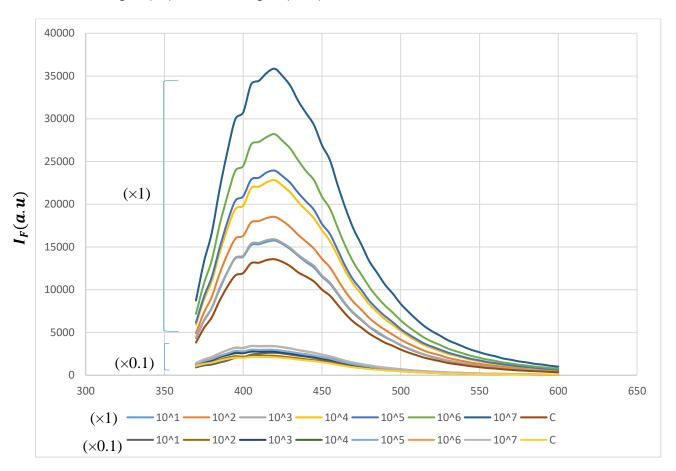


Figure 4.6 Fluorescence intensity (at 420nm) of Man-CQDs $(0.1\times)$ and E. coli ATCC 25922 in PBS

As expected, Man-CQDs was only able to label the strain of E. coli possessing FimH adhesin. Henceforward, we resumed the detection experiments with the appropriate strain; E. coli K12. Moreover, the relatively lower fluorescence intensity of Man-CQDs (×0.1), convinced us to repeat the detection tests with a more reliable and sensitive form of Man-CQDs. We, therefore, continued our detection tests with Man-CQDs (×1) to achieve higher fluorescence intensity difference and hence more certain results. To set a clearer vision, Figure 4.7 displays the fluorescence spectra of both Man-CQDs (×1) and Man-CQDs (×0.1) for the detection of E. coli K12.

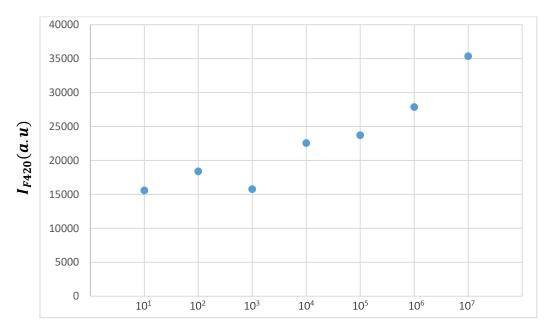


Wavelength (nm)

Figure 4.7 Fluorescence spectra of both Man-CQDs (×1) and Man-CQDs (×0.1) for the detection of E. coli K12 in PBS

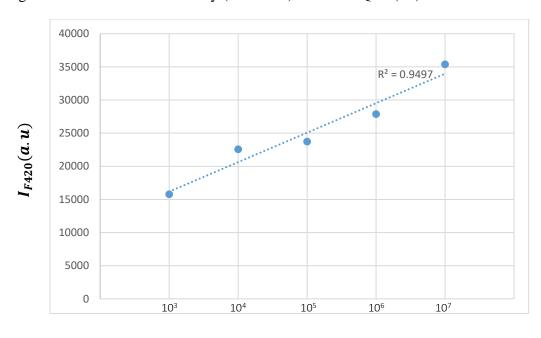
To better comprehend the results and the sensitivity of Man-CQDs (\times 1) as a probe to detect E. coli K12, the fluorescence intensity of Man-CQDs ($1\times$) and E. coli K12 at 420nm was derived from its fluorescence spectra. As shown in Figure 4.8 the displayed trend was much more desirable compare

to Figure 4.4 where the same conditions were applied with only Man-CQDs $(0.1\times)$ being the recognition element instead of Man-CQDs $(1\times)$.



E. Coli (CFU/mL)

Figure 4.8 Fluorescence intensity (at 420nm) of Man-CQDs (1×) and E. coli K12 in PBS



E. Coli (CFU/mL)

Figure 4.9 Fluorescence intensity (at 420nm) of Man-CQDs (1×) and E. coli K12 in PBS

Although Man-CQDs (\times 1) functioned more precisely and reliably than Man-CQDs (\times 0.1), it was noticed that the probe was not still sensitive enough to properly detect the concentrations below 1.0×10^3 . However, as illustrated in Figure 4.9 the fluorescence intensity followed a nice linear relationship with the logarithm of bacterial concentrations above 1.0×10^3 .

4.3 Repeatability, Reproducibility and Practicability of Man-CQDs

In order to examine the feasibility of employing this sensor in real life, the repeatability, reproducibility and practicability of Man-CQDs were evaluated. All the detection tests were carried out with Man-CQDs ($\times 1$) as the probe, E. coli K12 as the target pathogen and for the bacterial concentrations of 1.0×10^4 to 1.0×10^7 cfu/ml. The first series of tests were conducted with the same batch of the sensor on the same day in the standard PBS solution.

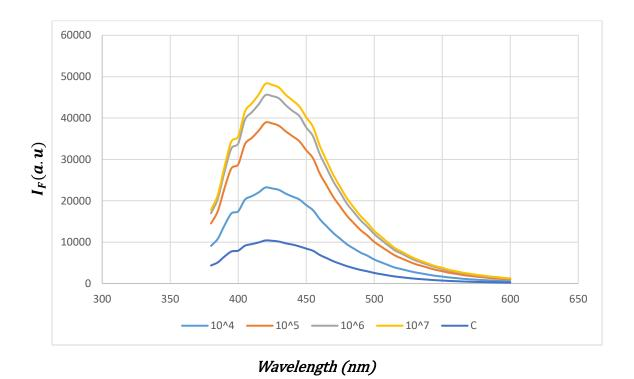


Figure 4.10 Fluorescence spectra of Man-CQDs (×1) for the detection of E. coli K12 in PBS

Series one: Same day - Same batch

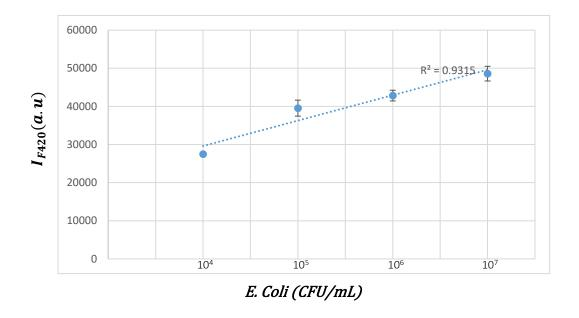


Figure 4.11 Fluorescence intensity (at 420nm) of Man-CQDs (1×) and E. coli K12 in PBS Series one: Same day - Same batch

The second series of tests were performed in PBS solution with the same batch of the sensor yet on different days. The third set of tests were done in PBS on the same day but with different batches of the sensor. It means that the sensors were being synthesized on different days. The results are presented in Figure 4.12 to Figure 4.15.

Relatively precise straight-line relationships were observed for all sets of detection tests (R^2 =0.936 and R^2 = 0.9963). However, the error bars showed dissimilar patterns. The relative standard deviations for the first series appear to be comparably low. This outcome was anticipated as the tests were all done on the same day and same Man-CQDs. The highest error bars were witnessed using different batches on the same day. This consequence may be due to an even fairly slight distinctness in quantum yields of the probes which were synthesized on different days. In series 2, as the concentration of E. coli decreased, the relative standard deviations increased. This trend is coherent as the detection proficiency ordinarily decreases in lower concentrations.

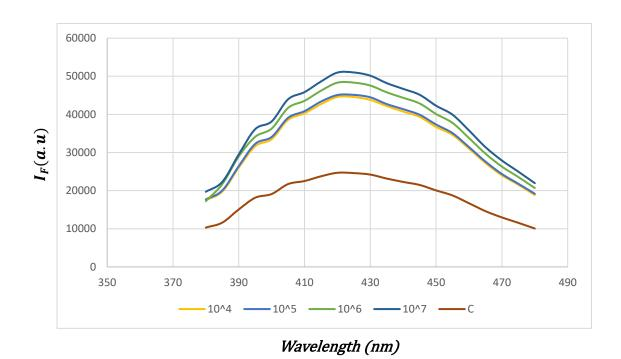


Figure 4.12 Fluorescence spectra of Man-CQDs (×1) for the detection of E. coli K12 in PBS Series two: Different days - Same batch

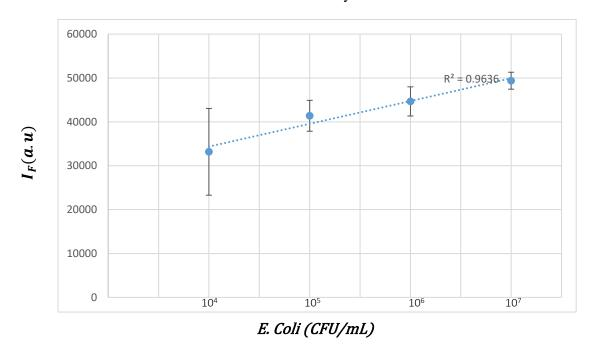


Figure 4.13 Fluorescence intensity (at 420nm) of Man-CQDs (1×) and E. coli K12 in PBS Series two: Different days - Same batch

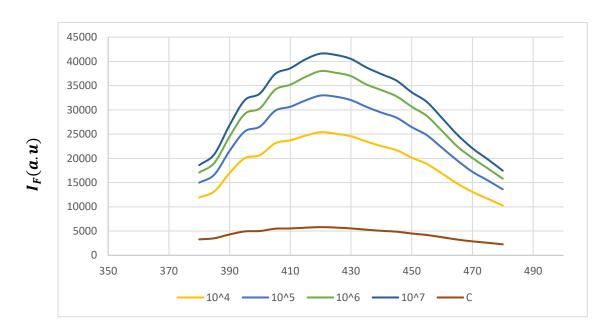


Figure 4.14 Fluorescence spectra of Man-CQDs (×1) for the detection of E. coli K12 in PBS

Series three: Same days – Different Batches

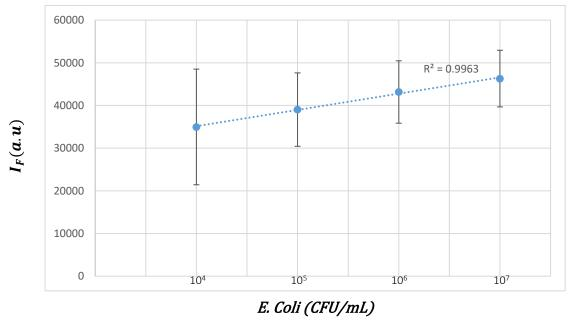


Figure 4.15 Fluorescence intensity (at 420nm) of Man-CQDs (1×) and E. coli K12 in PBS

Series three: Same days – Different Batches

The practicability of our synthesized sensor was assessed using various matrices such as tap water, apple juice and lemonade. The process by which the real samples were contaminated with E. coli K12 was explained in detail in chapter 3.

The spiked samples were then incubated with Man-CQDs (1×) at room temperature for 1 hour while gently being shaken. The procedure was followed by a 20 minutes centrifuge with a speed of 13000 RPM. Washing was an important step in order to remove free, non-attached Man-CQDs from the system. In the last measure, the bacterial residues were resuspended in the desirable medium. The detection tests for all three matrices were performed on the same day with the same batch whereas detection tests on different days with the same batch were also conducted for tap water. A similar relationship between the fluorescence intensity and the concentration of E. coli K12 was also observed in real-life samples. The following figures reveal the obtained results and confirm the rapid, inexpensive and simple Man-CQDs was accurately responsive in real-life samples.

Figure 4.16 and Figure 4.17 display the fluorescence spectra and fluorescence intensity of Man-CQDs $(1\times)$ and E. coli K12 in spiked tap water. The detection tests were performed multiple times on the same day and with the same batch of the probe. The detection tests illustrated in Figure 4.18 and Figure 4.19 were performed with Man-CQDs $(1\times)$ and E. coli K12 in spiked tap water multiple times on different days yet with the same batch of the probe.

It is essential to perform the detection tests with transparent pulp-free apple juice. The cloudy apple juice decreased the efficiency of our sensor. Not only it affected the optical properties of the final samples, but also its pulp got sedimented after being centrifuged. It was difficult to resuspend the bacterial pellets in the apple juice and the chance of free mannose being confined under these pulps increased and the final results were not reliable.

Figure 4.20 and Figure 4.21 show the fluorescence spectra and fluorescence intensity of Man-CQDs $(1\times)$ and E. coli K12 in spiked apple juice. The detection tests were performed multiple times on the same day and with the same batch of the sensor.

Figure 4.22 and Figure 4.23 illustrate the fluorescence spectra and fluorescence intensity of Man-CQDs $(1\times)$ and E. coli K12 in spiked lemonade. The detection tests were performed multiple times on the same day and with the same batch of Man-CQDs.

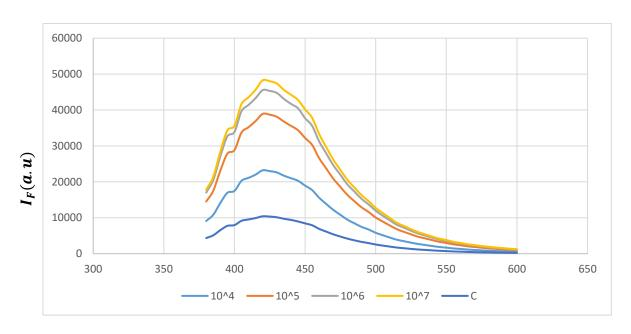


Figure 4.16 Fluorescence spectra of Man-CQDs $(\times 1)$ for the detection of E. coli K12 in Tap Water; Same day - Same batch

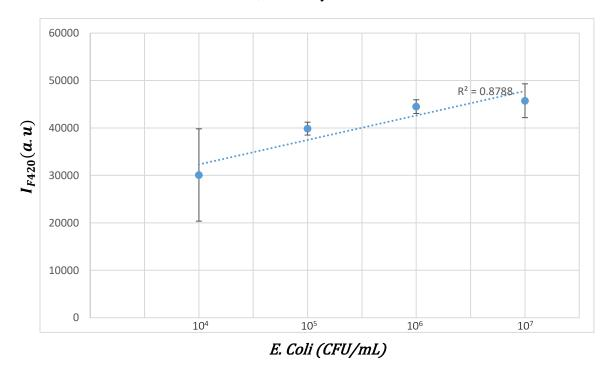


Figure 4.17 Fluorescence intensity (at 420nm) of Man-CQDs ($1\times$) and E. coli K12 in Tap Water; Same day - Same batch

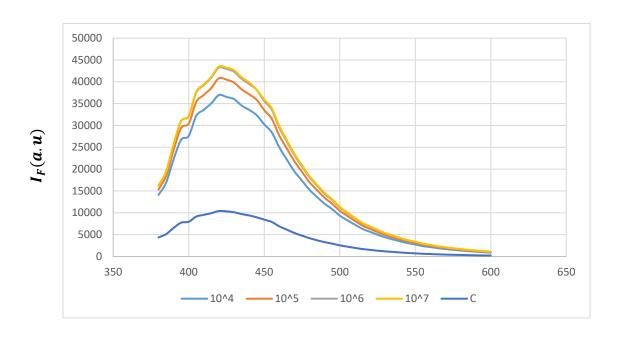


Figure 4.18 Fluorescence spectra of Man-CQDs $(\times 1)$ for the detection of E. coli K12 in Tap Water; Different days - Same batch

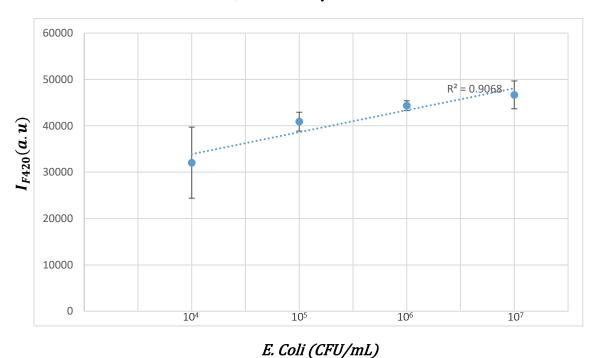


Figure 4.19 Fluorescence intensity (at 420nm) of Man-CQDs ($1\times$) and E. coli K12 in Tap Water; Different days - Same batch

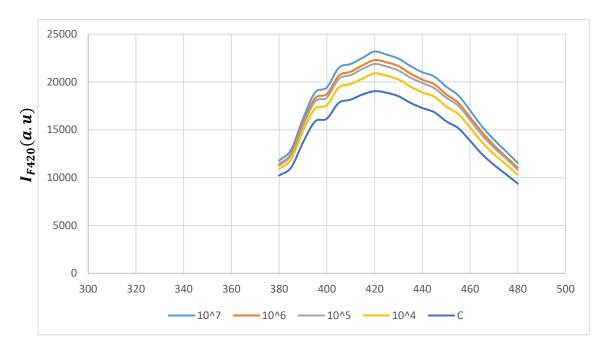


Figure 4.20 Fluorescence spectra of Man-CQDs $(\times 1)$ for the detection of E. coli K12 in Apple Juice; Same day - Same batch

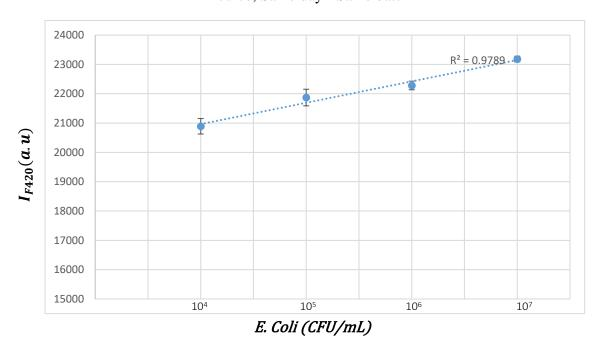


Figure 4.21 Fluorescence intensity (at 420nm) of Man-CQDs ($1\times$) and E. coli K12 in Apple Juice; Same day - Same batch

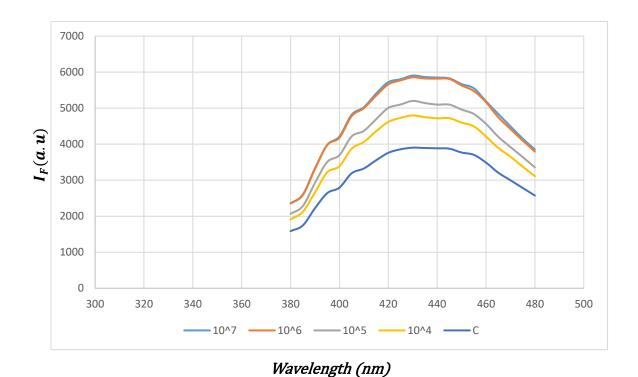


Figure 4.22 Fluorescence spectra of Man-CQDs $(\times 1)$ for the detection of E. coli K12 in Lemonade; Same day - Same batch

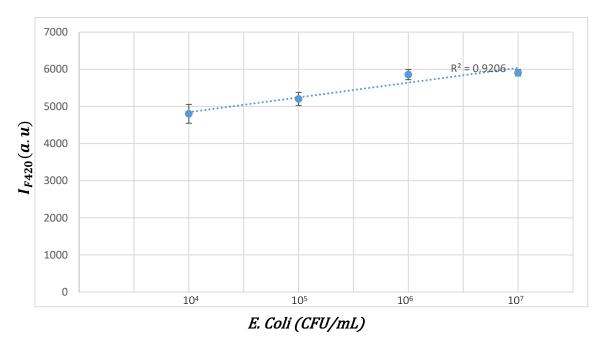
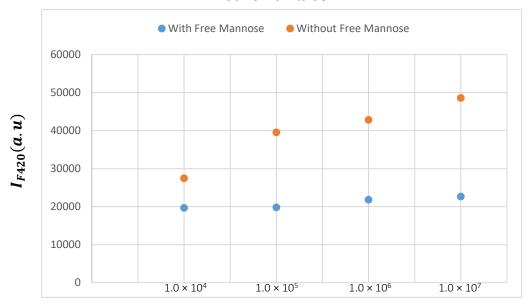


Figure 4.23 Fluorescence intensity (at 420nm) of Man-CQDs ($1\times$) and E. coli K12 in Lemonade; Same day - Same batch

4.4 The specificity of Man-CQDs to E. coli

A simple assessment was performed in order to approve the specificity of Mannose functionalized carbon quantum dots towards Escherichia coli. The detection tests were repeated with sensor 1 while the system was being nourished with either free mannose or free sucrose. The noticeably lower fluorescence intensity of the system containing free mannose reveals a significant decrease in binding efficiency of Man-CQDs towards E. coli.

Escherichia coli K12



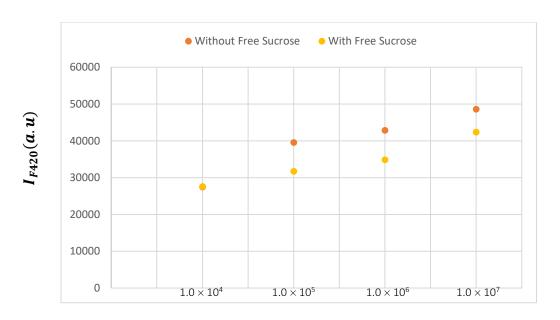
E. Coli (CFU/mL)

Figure 4.24 Fluorescence intensity (at 420nm) of Man-CQDs (1×) and E. coli K12 with and without free mannose

As it is clearly illustrated in Figure 4.24 the binding of Man-CQDs to FimH fimbriae was inhibited by mannose structures to a high extend. The same results were obtained for different concentrations of E. coli. The binding efficiency of the system being nourished with free mannose compared to the system without any free mannose being present has decreased by 53.38%, 49.03%, 49.97%, 28.38% for concentrations of 1.0×10^7 , 1.0×10^6 , 1.0×10^5 , 1.0×10^4 cfu/ml respectively. These

outcomes provide facts for our synthesized sensor particularity through E. coli. This judgement is much more reliable while considering the detection results of the other system carrying free sucrose. As illustrated in Figure 4.25 the binding inhibition caused by sucrose is relatively insignificant.

Escherichia coli K12



E. Coli (CFU/mL)

Figure 4.25 Fluorescence intensity (at 420nm) of Man-CQDs (1×) and E. coli K12 with and without free sucrose

The binding efficiency of the system being nourished with free sucrose compared to the system without any free sucrose nor free mannose being present, has decrease by 12.76%, 18.5%, 19.73%, 0.4% for concentrations of 1.0×10^7 , 1.0×10^6 , 1.0×10^5 , 1.0×10^4 cfu/ml respectively. As the presence of sucrose has a relatively minor effect on the detection efficiency of our sensor, we can conclude that the capacity of Man-CQDs for labeling Escherichia coli containing wild type fimbriae attribute to the strong and specific interaction between mannose structures of our sensor and type 1 fimbriae of E. coli K12.

4.5 E. coli labelling 4-Nitrophenyl α-D-mannopyranoside-CQDs

The obtained fluorescence spectra from bacterial detection with Man-CQDs in different matrices validated the possibility of using Man-CQDs for E. coli labelling. Although 1.0×10^4 cfu/ml is a satisfactory limit of detection regarding the simplicity and low cost of the probe, it is still notably higher than the acceptable limit of detection (LOD) required in food safety domains. Thus, our probe's sensitivity towards the target bacteria and subsequently its limit of detection needed to be improved. As it has already been explained in chapter 2, the introduction of certain side groups to mannose can increase its sensitivity towards FimH protein. Consequently, in order to increase the LOD of our probe, a derivative of mannose was chosen. 4-Nitrophenyl α -D-mannopyranoside was used which according to the literature demonstrated 50 times better affinity towards type 1 fimbriae than mannose.

The same previously-used method was repeated to synthesize 4-Nitrophenyl α -D-mannopyranoside-CQDs. The equal ratio of 20:1 was kept for ammonium citrate to 4-Nitrophenyl α -D-mannopyranoside. The mixture was heated up to 180 °C in an oven for 2 hours. The black residue was cooled to room temperature and dissolved in NaOH solution. The essential post-treatments were carried out as well. The maximum absorption of 4-Nitrophenyl α -D-mannopyranoside-CQDs was observed at 340 nm. It gets excited at 340 nm and emits at 420 nm. The absorption spectrum and fluorescence emission spectrum of 4-Nitrophenyl α -D-mannopyranoside-CQDs were identical to the ones for Man-CQDs which was formerly displayed in Figure 4.1 and Figure 4.2.

The detection tests in which 4-Nitrophenyl α -D-mannopyranoside-CQDs was used as the probe, were all conducted on E. coli K12. The aqueous 4-Nitrophenyl α -D-mannopyranoside-CQDs was employed as-synthesized (concentration \times 1) without any further dilutions.

As expected, 4-Nitrophenyl α -D-mannopyranoside-CQDs demonstrated a better limit of detection and happened to be a more sensitive probe. The fluorescence spectra and fluorescence intensity of 4-Nitrophenyl α -D-mannopyranoside-CQDs and E. coli K12 in PBS are shown in Figure 4.26 and Figure 27. The detection tests were performed multiple times on the same day and with the same batch of 4-Nitrophenyl α -D-mannopyranoside-CQDs for bacterial concentrations of 1.0×10^1 to 1.0×10^7 cfu/ml.

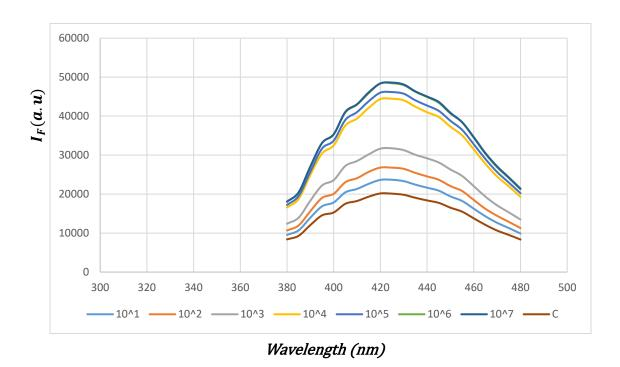


Figure 4.26 Fluorescence spectra of 4-Nitrophenyl α -D-mannopyranoside-CQDs for the detection of E. coli K12 in PBS; Same day - Same batch

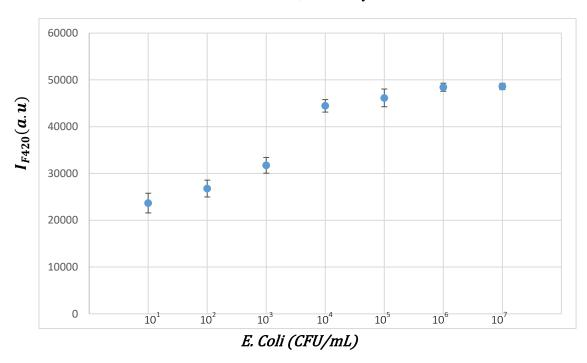


Figure 4.27 Fluorescence intensity (at 420nm) of 4-Nitrophenyl α -D-mannopyranoside-CQDs and E. coli K12 in PBS; Same day - Same batch

Figure 4.27 reveals a uniform relationship between the fluorescence intensity of 4-Nitrophenyl α -D-mannopyranoside-CQDs and E. coli K12 in PBS even for bacterial concentration below $1.0 \times$ 10⁴ cfu/ml. Figure 4.28 clarifies that the fluorescence intensity of our probe and target bacteria at 420nm demonstrates an almost perfect linear trend for concentrations of 1.0×10^1 to 1.0×10^3 cfu/ml.

The results obtained using 4-Nitrophenyl α-D-mannopyranoside-CQDs as a probe to detect E. coli K12 in PBS were very satisfactory, taking into account the straightforward and inexpensive nature of creating this sensor. 4-Nitrophenyl α-D-mannopyranoside is relatively more expensive than mannose, although it is still considerably cheaper than other recognition elements such as antibody and aptamer.

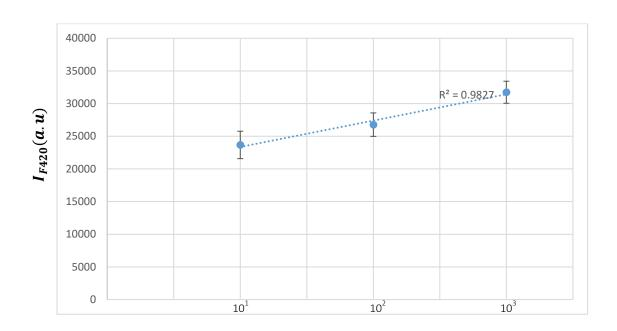


Figure 4.28 Fluorescence intensity (at 420nm) of 4-Nitrophenyl α-D-mannopyranoside-CQDs

and E. coli K12 in PBS; Same day - Same batch

E. Coli (CFU/mL)

4.6 Repeatability, Reproducibility and Practicability of 4-Nitrophenyl α -D-mannopyranoside-CQDs

To better evaluate the application of sensor 2 in E. coli detection, contaminated real-life samples were prepared and the results were assessed. The results suggest our rapid, relatively inexpensive and simple 4-Nitrophenyl α -D-mannopyranoside-CQDs demonstrates a considerable potential to be employed in the rapid screening of E. coli in real samples.

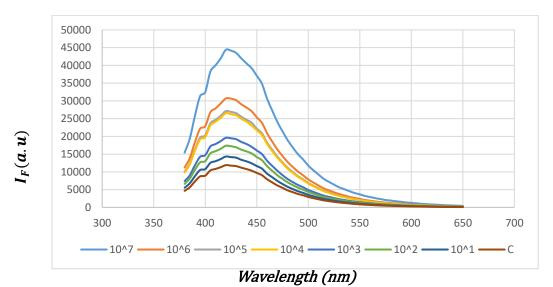


Figure 4.29 Fluorescence spectra of 4-Nitrophenyl α -D-mannopyranoside-CQDs for the detection of E. coli K12 in Tap Water. Same day - Same batch

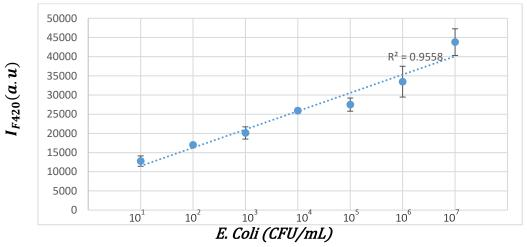


Figure 4.30 Fluorescence intensity (at 420nm) of 4-Nitrophenyl α -D-mannopyranoside-CQDs and E. coli K12 in Tap Water. Same day - Same batch

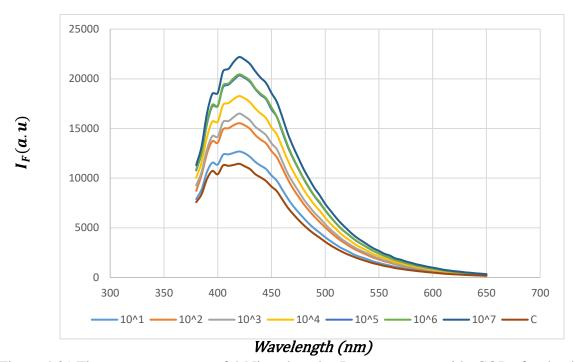


Figure 4.31 Fluorescence spectra of 4-Nitrophenyl α -D-mannopyranoside-CQDs for the detection of E. coli K12 in Apple Juice. Same day - Same batch

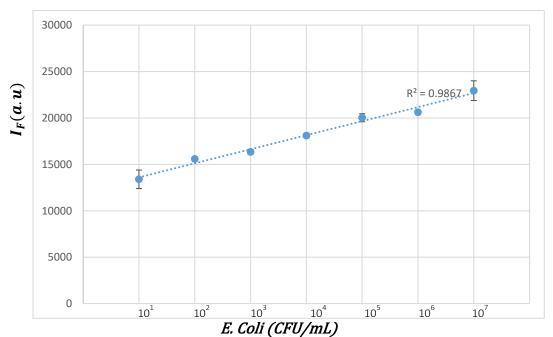


Figure 4.32 Fluorescence intensity (at 420nm) of 4-Nitrophenyl α-D-mannopyranoside-CQDs and E. coli K12 in Apple Juice. Same day - Same batch

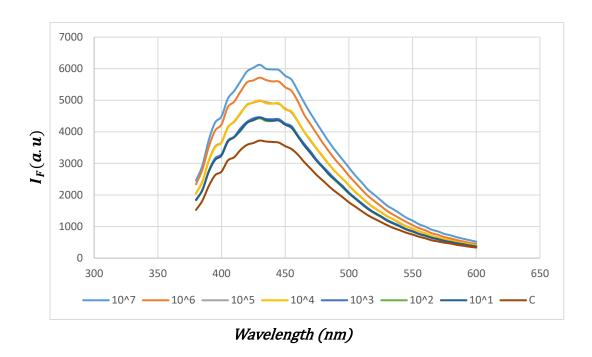


Figure 4.33 Fluorescence spectra of 4-Nitrophenyl α -D-mannopyranoside-CQDs for the detection of E. coli K12 in Lemonade. Same day - Same batch

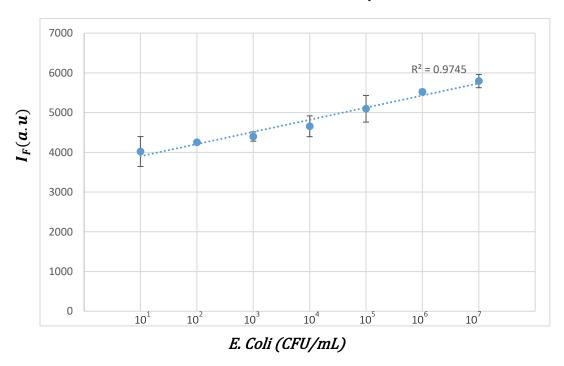


Figure 4.34 Fluorescence intensity (at 420nm) of 4-Nitrophenyl α -D-mannopyranoside-CQDs and E. coli K12 in Lemonade. Same day - Same batch

CHAPTER 5 GENERAL DISCUSSION

Both Man-CQDs as well as 4-Nitrophenyl α -D-mannopyranoside-CQDs demonstrated significant potentials to be used as detection elements in sensing Escherichia coli. The difference in fluorescence intensity of systems containing different bacterial concentrations provides an authentic route through which bacterial screening can be carried out. As it was displayed multiple times in the former chapter, the fluorescence intensity of the sample increased almost linearly upon the increase of bacterial concentration. So far, these probes can be taken into account more as qualitative sensors than quantitative ones. They can be employed in the rapid screening of E. coli in real samples. Applications in which the differences in E. coli concentrations in various samples require to be evaluated can exploit these relatively cheap and fast sensors.

Moreover, as the recognition process in both sensors is based on carbohydrate-protein adhesion, it is not possible to use these probes for certain E. coli strains which do not possess type 1 fimbriae. Adequate proteins and sufficient FimH adhesins are essential factors. Man-CQDs did not function properly with the samples containing E. coli ATCC 25922. The negative aspect of this situation is that the sensor can not be used for all the strains of E. coli and hence is not versatile. However, on the bright side, it should be mentioned that the life-threatening pathogenic E. coli O157:H7 which has been responsible for most of the E. coli outbreaks around the world, expresses wild type fimbriae and thus our probes are most probably effective enough to label it. Another important aspect to be discussed is the specificity of these probes to distinguish the target E. coli bacteria in a multi-organism matrix. Although FimH adhesins can principally be found in Escherichia coli, other microorganisms express this adhesin as well. For instance, the FimH adhesins in Klebsiella pneumoniae were aligned to FimH in Escherichia coli and they demonstrated 85% similarity in terms of the level of amino acid [82]. Further attempts can be concentrated on assessing the performance of our probes in environments that are contaminated by Klebsiella pneumoniae or other bacteria containing FimH. On the one hand, it is inspiring to be able to use these types of probes to detect other dangerous pathogenic bacteria; On the other hand, it affects the sensor's specificity and increases the possibility of false-positive results in multi-organism matrices.

Another valuable resolution that was stated in this chapter is the fact that the non-diluted solution of Man-CQDs showed to be a relatively more effective probe. Man-CQDs ($\times 0.1$) was 10 times

more diluted than the Man-CQDs ($\times 1$) solution and hence the fluorescence intensity of the samples tested with Man-CQDs ($\times 1$) was higher in comparison to the ones with Man-CQDs ($\times 0.1$). This results in greater differences in the fluorescence intensity of different samples containing different bacterial concentrations. The aforementioned factors signify Man-CQDs ($\times 1$) as a more accurate sensor. It is also beneficial to figure out if an optimal concentration for Man-CQDs exists.

Although Man-CQDs (×1) properly functioned in E. coli K12 recognition even in various matrices, it does not display enough sensitivity to distinguish bacterial concentration below 1.0×10^4 cfu/ml. Considering the fact that based on the quantitative risk assessment of previous outbreak of E. coli O157:H7-associated illness, the irresistible amount of Escherichia coli O157:H7 responsible for the infection has been evaluated between 10 to 100 cfu/ml in food samples, 1.0×10^4 cfu/ml is noticeably a high limit of detection for food packaging purposes. 4-Nitrophenyl α -D-mannopyranoside-CQDs on the other hand was sensitive enough to label the bacterial concentrations even as low as 1.0×10^1 cfu/ml. The comparably lower error bars in the detection systems where 4-Nitrophenyl α -D-mannopyranoside-CQDs acted as the probe, magnify the prospective potential of this sensor to be used in E. coli screening in suspected contaminated food.

A vital aspect that must be considered in the final applications and if these probes are safe to be in contact with food. Mannose, the natural substrate that this study was established on, contains non-toxic molecules and is commercially used as food sweeteners. Mannose is even available in form of pills and can be used either for an inherited disorder named carbohydrate-deficient glycoprotein syndrome type 1b or for infections of the kidney, bladder or urethra. 4-Nitrophenyl α -D-mannopyranoside needs further investigation. It is recommended to handle its plain powder with personal protective equipment as it should not be breathed. It is worth mentioning that 4-Nitrophenyl α -D-mannopyranoside is considered as one of the main novel elements in water filtration mats therefore the possibility of using it for food samples is not unattainable. Carbon quantum dots also require to undergo specific examination in order to be approved to be used in contact with food. To be brief, although 4-Nitrophenyl α -D-mannopyranoside-CQDs has demonstrated to be a more sensitive sensor, its safety to be exploited in the food industry requires further investigations. Other applications could also be considered since bacterial detection is required and beneficial in so many other industries such as cosmetics, pharmaceuticals, medical device manufacturers, health care facilities, etc.

5.1 The necessity of the quenching mechanism

The main goal of this study was to introduce a potential sensor to be used for the detection of pathogenic Escherichia coli in contaminated food. The ultimate idea is to capture this sensor on a solid surface and eventually assemble it on food packaging. Few challenges must be confronted in advance in order to achieve this objective. The main problem though is not related to how the sensor should get attached to the surface but in fact, how it is going to accurately function on a solid surface. In order to overcome this issue, it is required to fully understand the mechanism through which either Man-CQDs or 4-Nitrophenyl α -D-mannopyranoside-CQDs screen E. coli.

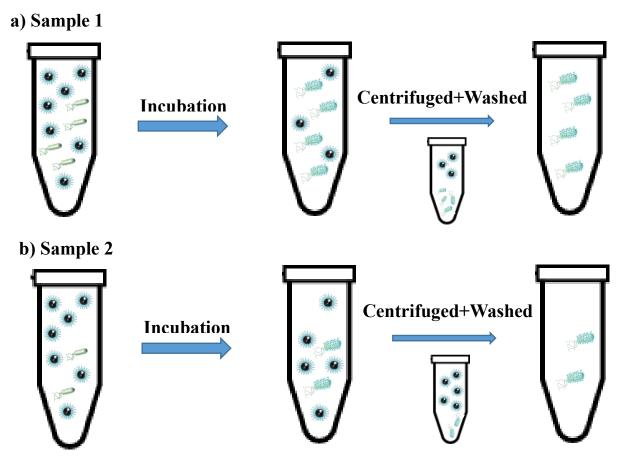


Figure 5.1 Detection mechanism in a liquid-based probe a) sample 1: detection procedure for a sample containing a higher concentration of E. coli. b) sample 2: detection procedure for a sample containing a lower concentration of E. coli.

Let's consider sample 1 and 2 are incubated with the same amount of probe for 1 hour under gentle shaking at room temperature. The incubation provides the required situation for the probe's elements to target E. coli and adhere to them by the means of carbohydrates-protein attachment. Two case scenarios are illustrated above in Figure 5.1. Figure 5.1 a displays scenario one where sample 1 with a relatively higher concentration of E. coli is being detected while in Figure 5.1 b, sample 2 contains a lower concentration of target bacteria. Both scenarios are happening in a liquid phase. Likewise, centrifuged and washed, therefore the free mannose is being removed. At the end of this simple procedure, sample 1, containing a higher concentration of E. coli demonstrate higher fluorescence intensity while sample 2 displays lower fluorescence intensity. We can then conclude the sample expressing higher fluorescence intensity, has carried higher E. coli concentration from the beginning.

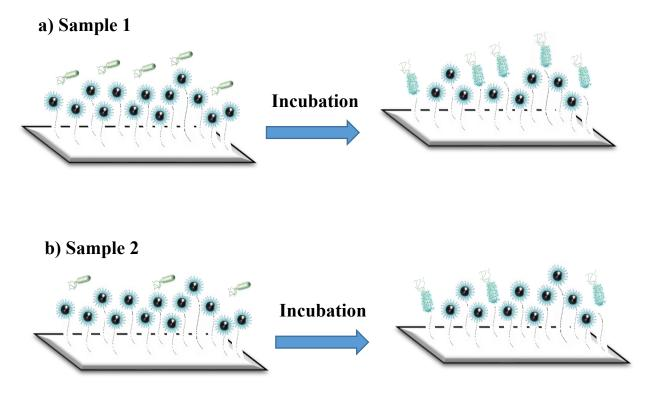


Figure 5.2 Detection mechanism in a solid-based probe a) sample 1: detection procedure for a sample containing a higher concentration of E. coli. b) sample 2: detection procedure for a sample containing a lower concentration of E. coli.

Otherwise, changing from a liquid-based probe to a probe attached to a solid surface induce more complexity in terms of detection mechanism. Figure 5.2 displays the same scenarios but for a solid based sensor.

Imagine the illustrated solid surfaces that have been previously modified and attached to either of our synthesized sensors. Figure 5.2 explains why the same previously-efficient detection mechanism is not practical to be used for a solid based probe. Both Sample 1 and sample 2, as illustrated in Figure 5.2 a and Figure 5.2 b, are incubated with the solid-based probes for the same amount of time and under similar conditions. Both solid-based probes contain the same numbers of functionalized CQDs and yet display similar fluorescent intensity prior to the incubation. After incubation, in sample 1 which accommodates a higher concentration of E. coli, more bacteria have been attached to the probe while in sample 2, due to lower bacterial concentration, fewer E. coli have been stuck to the sensor. In this step the fluorescent intensity of both samples is still the same as the number of functionalized CQDs together with functionalized CQDs labelling E. coli stay the same. Owing to the non-attached probes in a liquid-phase sensor, centrifuge and washing were two important and essential steps to remove free non-attached functionalized CQDs. As this is not the case in solid-based probes, it is then highly required to figure out a theoretically efficient way to solve this limitation before switching the phases. The proposed solution is to exploit a proper quenching agent. The general concept of quenching and its possible mechanisms have been covered in chapter 2. The usefulness of including a suitable quenching mechanism in this study, for bacterial detection with a solid-based prob, is plainly demonstrated in Figure 5.3.

Once more, two case scenarios are displayed. Unlike the previously described system, this system includes an appropriate quenching agent by which the fluorescent properties of the sensors, solid surfaces modified with functionalized CQDs, are initially disabled. Not only should the proper quenching agent be able to effectively quench the functionalized CQDs, but also it has to have a lower affinity towards functionalized CQDs compared to FimH. The second condition is also essential considering that the quenching agent should be replaced with E. coli in the incubation step. This replacement causes the fluorescent properties of functionalized CQDs to be enabled again. Through this method, after the incubation step, sample 1 displayed in Figure 5.3 a which contains higher bacterial concentration demonstrates higher fluorescent intensity compared to sample 2, Figure 5.3 b, which carries fewer colonies of E. coli. The difference in the fluorescent

intensity of these two samples is the key feature in bacterial detection and could be provided by the help of a quenching mechanism,

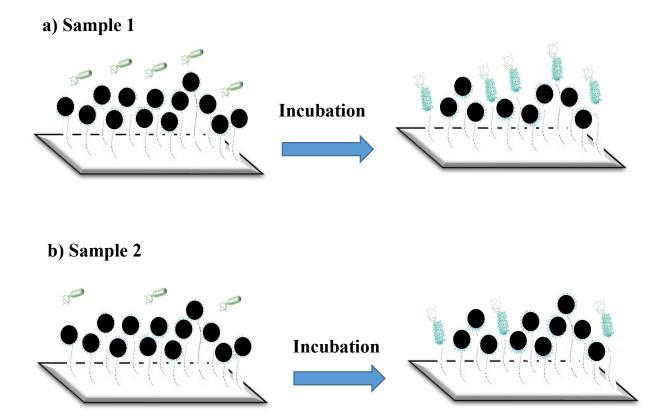


Figure 5.3 Detection mechanism in a solid-based probe with quenching mechanism a) sample 1: detection procedure for a sample containing a higher concentration of E. coli. b) sample 2: detection procedure for a sample containing a lower concentration of E. coli.

This study was mainly focused on liquid phase. We wanted to be assured that the sensors can effectively label E. coli in liquid systems before investigating a solid based sensor. The basic of quenching mechanism and its importance have been fully discussed to be used in future works.

CHAPTER 6 CONCLUSION AND RECOMMENDATION

In this work, we have demonstrated two E. coli sensors that function based on carbohydrate-protein interactions. Both sensors are liquid based probes and currently can only be used to detect E. coli in liquid systems. They are both effective on certain strains of Escherichia coli which contain type 1 fimbriae. Both sensors were responsive in real life contaminated samples. The limit of detection for Man-CQDs is 10^4 cfu while the LOD of 4-Nitrophenyl α -D-mannopyranoside-CQDs is above 10^1 cfu.

For future works, it is recommended to discover a proper quenching agent. The necessity of employing a quenching mechanism has been fully explained in chapter 5. It is the first step to achieve the ultimate goal which is to proceed from a liquid-based sensor to a solid based one. A suitable quenching agent is also highly advantageous in liquid phase detections as it eliminates the need for washing step and hence minimizes the inaccuracy of the sensor.

Unlike many other master's projects, this study will affect human lives in reality. By overcoming the complications related to implementing the sensors on solid based surfaces, we can ultimately introduce a life-changing biosensor on food packaging which not only will improve the world-wide health situation, but also benefits several industries.

REFERENCES

- 1. Wang, Y., et al., Monitoring of Escherichia coli O157:H7 in food samples using lectin based surface plasmon resonance biosensor. Food Chemistry, 2013. **136**(3): p. 1303-1308.
- 2. CNN. *E. Coli Outbreaks Fast Facts*. June 17, 2020; Available from: https://www.cnn.com/2013/06/28/health/e-coli-outbreaks-fast-facts/index.html.
- 3. Yazgan, I., et al., *Biosensor for selective detection of E. coli in spinach using the strong affinity of derivatized mannose with fimbrial lectin.* Biosens Bioelectron, 2014. **61**: p. 266-73.
- 4. Disney, M.D. and P.H. Seeberger, *The Use of Carbohydrate Microarrays to Study Carbohydrate-Cell Interactions and to Detect Pathogens*. Chemistry & Biology, 2004. **11**(12): p. 1701-1707.
- 5. Ofek, I. and E.H. Beachey, *Mannose Binding and Epithelial Cell Adherence of Escherichia coli*. Infection and Immunity, 1978. **22**(1): p. 247.
- 6. Lin, C.-C., et al., Selective Binding of Mannose-Encapsulated Gold Nanoparticles to Type 1 Pili in Escherichia coli. Journal of the American Chemical Society, 2002. **124**(14): p. 3508-3509.
- 7. S. Thomas, P.M.V.a.A.P.M., *Advances in natural polymers*. 2012, London: Springer.
- 8. Weng, C.-I., et al., *One-step synthesis of biofunctional carbon quantum dots for bacterial labeling*. Biosensors and Bioelectronics, 2015. **68**: p. 1-6.
- 9. Call, D.R., M.K. Borucki, and F.J. Loge, *Detection of bacterial pathogens in environmental samples using DNA microarrays*. Journal of Microbiological Methods, 2003. **53**(2): p. 235-243.
- 10. Organization, W.H. *Ten threats to global health in 2019*. 2019; Available from: https://www.who.int/vietnam/news/feature-stories/detail/ten-threats-to-global-health-in-2019.
- 11. Mead, P.S., et al., *Food-related illness and death in the United States*. Emerging infectious diseases, 1999. **5**(5): p. 607-625.
- 12. Lim, J.Y., J. Yoon, and C.J. Hovde, *A brief overview of Escherichia coli O157:H7 and its plasmid O157*. Journal of microbiology and biotechnology, 2010. **20**(1): p. 5-14.
- 13. Nataro, J.P. and J.B. Kaper, *Diarrheagenic Escherichia coli*. Clinical Microbiology Reviews, 1998. **11**(1): p. 142.
- 14. Riley, L.W., et al., *Hemorrhagic Colitis Associated with a Rare Escherichia coli Serotype*. New England Journal of Medicine, 1983. **308**(12): p. 681-685.
- 15. Wells, J.G., et al., Laboratory investigation of hemorrhagic colitis outbreaks associated with a rare Escherichia coli serotype. Journal of Clinical Microbiology, 1983. **18**(3): p. 512.
- 16. Frenzen, P.D., et al., *Economic Cost of Illness Due to Escherichia coli O157 Infections in the United States*. Journal of Food Protection, 2005. **68**(12): p. 2623-2630.

- 17. Rangel, J.M., et al., *Epidemiology of Escherichia coli O157:H7 outbreaks*, *United States*, 1982-2002. Emerging infectious diseases, 2005. **11**(4): p. 603-609.
- 18. Meng, J. and M.P. Doyle, *Emerging and evolving microbial foodborne pathogens*. Bulletin de l'Institut Pasteur, 1998. **96**(3): p. 151-163.
- 19. Kaspar, C.W. and C. Tartera, 16 Methods for Detecting Microbial Pathogens in Food and Water, in Methods in Microbiology, R. Grigorova and J.R. Norris, Editors. 1990, Academic Press. p. 497-531.
- 20. Meng, J., et al., *Polymerase chain reaction for detecting Escherichia coli O157:H7*. International Journal of Food Microbiology, 1996. **32**(1): p. 103-113.
- 21. Ivnitski, D., et al., *Biosensors for detection of pathogenic bacteria*. Biosensors and Bioelectronics, 1999. **14**(7): p. 599-624.
- 22. Ge, B., et al., A PCR-ELISA for detecting Shiga toxin-producing Escherichia coli. Microbes and Infection, 2002. **4**(3): p. 285-290.
- 23. Yamaguchi, N., et al., *Rapid detection of respiring Escherichia coli 0157:H7 in apple juice, milk, and ground beef by flow cytometry.* Cytometry Part A, 2003. **54A**(1): p. 27-35.
- 24. Call, D.R., M.K. Borucki, and F.J. Loge, *Detection of bacterial pathogens in environmental samples using DNA microarrays.* J Microbiol Methods, 2003. **53**(2): p. 235-43.
- 25. Tseng, Y.-T., et al., *Preparation of highly luminescent mannose–gold nanodots for detection and inhibition of growth of Escherichia coli*. Biosensors and Bioelectronics, 2011. **27**(1): p. 95-100.
- 26. Disney, M.D., et al., *Detection of Bacteria with Carbohydrate-Functionalized Fluorescent Polymers*. Journal of the American Chemical Society, 2004. **126**(41): p. 13343-13346.
- 27. Yu, L.S.L., S.A. Reed, and M.H. Golden, *Time-resolved fluorescence immunoassay* (TRFIA) for the detection of Escherichia coli O157:H7 in apple cider. Journal of Microbiological Methods, 2002. **49**(1): p. 63-68.
- 28. Torun, Ö., et al., *Comparison of sensing strategies in SPR biosensor for rapid and sensitive enumeration of bacteria*. Biosensors and Bioelectronics, 2012. **37**(1): p. 53-60.
- 29. Teunis, P., K. Takumi, and K. Shinagawa, *Dose response for infection by Escherichia coli O157:H7 from outbreak data*. Risk Anal, 2004. **24**(2): p. 401-7.
- 30. Michael T. Madigan, J.M.M., Kelly S. Bender, Daniel H. Buckley, David Stahl, *Brock Biology of Microorganisms*. 14th edition ed. 2014: Pearson.
- 31. Evanko, D., Measuring a bacteria's sweet tooth. Nature Methods, 2005. **2**(2): p. 88-89.
- 32. Pieters, R.J., *Intervention with bacterial adhesion by multivalent carbohydrates*. Med Res Rev, 2007. **27**(6): p. 796-816.
- 33. Sachdeva, G., et al., *SPAAN: a software program for prediction of adhesins and adhesin-like proteins using neural networks.* Bioinformatics, 2005. **21**(4): p. 483-491.
- 34. Flint, J., et al., *Ligand-mediated Dimerization of a Carbohydrate-binding Module Reveals a Novel Mechanism for Protein–Carbohydrate Recognition.* Journal of Molecular Biology, 2004. **337**(2): p. 417-426.

- 35. Critchley, P., et al., Carbohydrate-protein interactions at interfaces: synthesis of thiolactosyl glycolipids and design of a working model for surface plasmon resonance. Organic & Biomolecular Chemistry, 2003. 1(6): p. 928-938.
- 36. Pedroso, M.M.a.W., Ailton M. and Roque-Barreira, Maria Cristina and Bueno, Paulo R. and Faria, Ronaldo C., *Quartz Crystal Microbalance monitoring the real-time binding of lectin with carbohydrate with high and low molecular mass*. Microchemical Journal, 2008. **89**(2): p. 153-158.
- 37. Honda, P.T., Capillary Electrophoresis of Carbohydrates, in Methods in Molecular Biology. Humana Press.
- 38. Knill, C.J. and J.F. Kennedy, *NMR Spectroscopy of Glycoconjugates: J. Jiménez-Barbero, T. Peters (Eds.); Wiley-VCH, Weinheim, 2003, xv+320 pages, ISBN 3-527-30414-2, (£80.00).* Carbohydrate Polymers, 2004. **56**(3): p. 371.
- 39. Lee, Y.C., Fluorescence Spectrometry in Studies of Carbohydrate-Protein Interactions. The Journal of Biochemistry, 1997. **121**(5): p. 818-825.
- 40. Zeng, X., et al., *Carbohydrate–protein interactions and their biosensing applications*. Analytical and Bioanalytical Chemistry, 2012. **402**(10): p. 3161-3176.
- 41. Kunz, C., et al., *Oligosaccharides in human milk: structural, functional, and metabolic aspects.* Annu Rev Nutr, 2000. **20**: p. 699-722.
- 42. Hu, X., et al., *d-Mannose: Properties, Production, and Applications: An Overview.* Comprehensive Reviews in Food Science and Food Safety, 2016. **15**(4): p. 773-785.
- 43. Chen, F.-E., et al., *An improved synthesis of a key intermediate for* (+)-biotin from *D-mannose*. Carbohydrate research, 2007. **342**(16): p. 2461-2464.
- 44. Chen, L.-G.a.L., Zhi-Lan and Zhuo, Ren-Xi, Synthesis and properties of degradable hydrogels of konjac glucomannan grafted acrylic acid for colon-specific drug delivery. Polymer, 2005. **46**: p. 6274-6281.
- 45. Stahlhut, S.G., et al., Comparative Structure-Function Analysis of Mannose-Specific FimH Adhesins from Klebsiella pneumoniae and Escherichia coli. Journal of Bacteriology, 2009. **191**(21): p. 6592.
- 46. Krogfelt, K.A., H. Bergmans, and P. Klemm, *Direct evidence that the FimH protein is the mannose-specific adhesin of Escherichia coli type 1 fimbriae*. Infection and immunity, 1990. **58**(6): p. 1995-1998.
- 47. Ponniah, S., et al., Fragmentation of Escherichia coli type 1 fimbriae exposes cryptic D-mannose-binding sites. Journal of bacteriology, 1991. **173**(13): p. 4195-4202.
- 48. Jones, C.H., et al., FimH adhesin of type 1 pili is assembled into a fibrillar tip structure in the Enterobacteriaceae. Proceedings of the National Academy of Sciences of the United States of America, 1995. **92**(6): p. 2081-2085.
- 49. Dong, H., et al., *Biofunctionalized Cellulose Nanofibrils Capable of Capture and Antiadhesion of Fimbriated Escherichia coli*. ACS Applied Bio Materials, 2019. **2**(7): p. 2937-2945.

- 50. Bouckaert, J., et al., Receptor binding studies disclose a novel class of high-affinity inhibitors of the Escherichia coli FimH adhesin. Molecular Microbiology, 2005. **55**(2): p. 441-455.
- 51. Lindhorst, T.K., et al., *Effect of p-Substitution of Aryl α-D-Mannosides on Inhibiting Mannose-Sensitive Adhesion of Escherichia coli Syntheses and Testing*. European Journal of Organic Chemistry, 1998. **1998**(8): p. 1669-1674.
- 52. Geys, J., et al., *Acute toxicity and prothrombotic effects of quantum dots: impact of surface charge.* Environmental health perspectives, 2008. **116**(12): p. 1607-1613.
- 53. Lim, S.Y., W. Shen, and Z. Gao, *Carbon quantum dots and their applications*. Chemical Society Reviews, 2015. **44**(1): p. 362-381.
- 54. Wang, Y. and A. Hu, *Carbon quantum dots: synthesis, properties and applications.* Journal of Materials Chemistry C, 2014. **2**(34): p. 6921-6939.
- 55. Xu, X., et al., *Electrophoretic Analysis and Purification of Fluorescent Single-Walled Carbon Nanotube Fragments*. Journal of the American Chemical Society, 2004. **126**(40): p. 12736-12737.
- 56. Sun, Y.-P., et al., *Quantum-Sized Carbon Dots for Bright and Colorful Photoluminescence*. Journal of the American Chemical Society, 2006. **128**(24): p. 7756-7757.
- 57. Li, H., et al., *Water-Soluble Fluorescent Carbon Quantum Dots and Photocatalyst Design*. Angewandte Chemie International Edition, 2010. **49**(26): p. 4430-4434.
- 58. Liu, Y., C.-y. Liu, and Z.-y. Zhang, *Synthesis and surface photochemistry of graphitized carbon quantum dots.* Journal of Colloid and Interface Science, 2011. **356**(2): p. 416-421.
- 59. Demchenko, A.P. and M.O. Dekaliuk, *Novel fluorescent carbonic nanomaterials for sensing and imaging*. Methods and Applications in Fluorescence, 2013. **1**(4): p. 042001.
- 60. Rimal, V., S. Shishodia, and P.K. Srivastava, *Novel synthesis of high-thermal stability carbon dots and nanocomposites from oleic acid as an organic substrate*. Applied Nanoscience, 2020. **10**(2): p. 455-464.
- 61. Zhou, J., et al., An Electrochemical Avenue to Blue Luminescent Nanocrystals from Multiwalled Carbon Nanotubes (MWCNTs). Journal of the American Chemical Society, 2007. **129**(4): p. 744-745.
- 62. Liu, R., et al., An aqueous route to multicolor photoluminescent carbon dots using silica spheres as carriers. Angew Chem Int Ed Engl, 2009. **48**(25): p. 4598-601.
- 63. Bourlinos, A.B., et al., Surface Functionalized Carbogenic Quantum Dots. 2008. **4**(4): p. 455-458.
- 64. Zhu, H., et al., *Microwave synthesis of fluorescent carbon nanoparticles with electrochemiluminescence properties.* Chemical Communications, 2009(34): p. 5118-5120.
- 65. Oza, G., et al., A Green Route Towards Highly Photoluminescent and Cytocompatible Carbon dot Synthesis and its Separation Using Sucrose Density Gradient Centrifugation. Journal of Fluorescence, 2015. **25**(1): p. 9-14.

- 66. Phadke, C., et al., *Biogenic Synthesis of Fluorescent Carbon Dots at Ambient Temperature Using Azadirachta indica (Neem) gum.* Journal of Fluorescence, 2015. **25**(4): p. 1103-1107.
- 67. Nicollian, E.H., Surface Passivation of Semiconductors. 1971. **8**(5): p. S39-S49.
- 68. Molaei, M.J., Carbon quantum dots and their biomedical and therapeutic applications: a review. RSC advances, 2019. **9**(12): p. 6460-6481.
- 69. Feng, H. and Z. Qian, Functional Carbon Quantum Dots: A Versatile Platform for Chemosensing and Biosensing. The Chemical Record, 2018. **18**(5): p. 491-505.
- 70. Wang, N., et al., Green preparation of carbon dots with papaya as carbon source for effective fluorescent sensing of Iron (III) and Escherichia coli. Biosens Bioelectron, 2016. **85**: p. 68-75.
- 71. Lai, I.P.-J., et al., *Solid-state synthesis of self-functional carbon quantum dots for detection of bacteria and tumor cells.* Sensors and Actuators B: Chemical, 2016. **228**: p. 465-470.
- 72. Quenching of Fluorescence, in Principles of Fluorescence Spectroscopy, J.R. Lakowicz, Editor. 2006, Springer US: Boston, MA. p. 277-330.
- 73. Hao, T., et al., An eco-friendly molecularly imprinted fluorescence composite material based on carbon dots for fluorescent detection of 4-nitrophenol. Microchimica Acta, 2016. **183**(7): p. 2197-2203.
- 74. Baker, S.N. and G.A. Baker, *Luminescent Carbon Nanodots: Emergent Nanolights*. 2010. **49**(38): p. 6726-6744.
- 75. Iqbal, A., et al., Carbon dots prepared by solid state method via citric acid and 1,10-phenanthroline for selective and sensing detection of Fe2+ and Fe3+. Sensors and Actuators B: Chemical, 2016. 237: p. 408-415.
- 76. Zu, F., et al., *The quenching of the fluorescence of carbon dots: A review on mechanisms and applications.* Microchimica Acta, 2017. **184**(7): p. 1899-1914.
- 77. Liu, H., et al., *Interaction between fluorescein isothiocyanate and carbon dots: Inner filter effect and fluorescence resonance energy transfer.* Spectrochimica Acta Part A: Molecular and Biomolecular Spectroscopy, 2017. **171**: p. 311-316.
- 78. Wang, X., et al., *Highly sensitive and selective aptasensor for detection of adenosine based on fluorescence resonance energy transfer from carbon dots to nano-graphite*. Journal of colloid and interface science, 2017. **508**: p. 455-461.
- 79. Purbia, R. and S. Paria, A simple turn on fluorescent sensor for the selective detection of thiamine using coconut water derived luminescent carbon dots. Biosensors and Bioelectronics, 2016. **79**: p. 467-475.
- 80. Mishra, S.K., S. Bhardwaj, and B.D. Gupta, Surface Plasmon Resonance-Based Fiber Optic Sensor for the Detection of Low Concentrations of Ammonia Gas. IEEE Sensors Journal, 2015. **15**(2): p. 1235-1239.
- 81. Shi, D., et al., *P-doped carbon dots act as a nanosensor for trace 2,4,6-trinitrophenol detection and a fluorescent reagent for biological imaging.* RSC Advances, 2015. **5**(119): p. 98492-98499.

82. Stahlhut, S.G., et al., Comparative structure-function analysis of mannose-specific FimH adhesins from Klebsiella pneumoniae and Escherichia coli. Journal of bacteriology, 2009. **191**(21): p. 6592-6601.